Divergent receptor proteins confer responses to different karrikins in two ephemeral weeds

Yueming Kelly Sun[1,2], Adrian Scaffidi[1], Jiaren Yao[1], Kim Melville[1], Steven M Smith[3,4], Gavin R Flematti[1] and Mark T Waters[1,2,5]

1. School of Molecular Sciences, The University of Western Australia, 35 Stirling Hwy, Perth, WA 6009, Australia
2. Australian Research Council Centre of Excellence in Plant Energy Biology, The University of Western Australia, 35 Stirling Hwy, Perth, WA 6009, Australia
3. School of Natural Sciences, The University of Tasmania, Hobart, TAS 7000, Australia
4. Institute of Genetics and Developmental Biology, Chinese Academy of Sciences, 1 West Beichen Road, Beijing 100101, PR China.
5. Author for correspondence: mark.waters@uwa.edu.au

Word count (Abstract and main text): 2396 words

Abstract

Seed germination is responsive to environmental chemical cues, such as karrikins, which are germination stimulants produced from wildfires[1,2]. Seeds of *Brassica tournefortii* – a widespread problematic weed associated with post-fire and disturbance sites – are highly sensitive to KAR_1, the most abundant karrikin, whereas *Arabidopsis thaliana* responds more sensitively to KAR_2, a less abundant karrikin[3,4]. The mechanism for these differential responses is unclear. KARRIKIN INSENSITIVE2 (KAI2), a paralogue of the strigolactone receptor DWARF14 (D14), is the putative karrikin receptor identified from *Arabidopsis*[4,5]. Here we show that *B. tournefortii* exhibits greater sensitivity for KAR_1 relative to KAR_2 in multiple biological assays. We demonstrate that *B. tournefortii* differentially expresses three *KAI2* homologues, two of which rescue the *Arabidopsis kai2-2* null mutant. Notably, the most abundantly expressed homologue in *B. tournefortii* is sufficient to confer enhanced responses to KAR_1 relative to KAR_2 when expressed in *Arabidopsis*. We further identify two variant amino acid residues that support differential ligand preferences between the two *B. tournefortii* homologues. Our findings provide clear evidence that KAI2 is the receptor for karrikins, since specific amino acid substitutions near the active site change ligand specificity. Our results also suggest that duplication and diversification of KAI2 proteins could provide weedy ephemerals with the ability to respond sensitively to different karrikins or related compounds produced by environmental disturbance.

Main

Recovery of vegetation after wildfires results in part from the germination of dormant seed in the soil. Plant-derived smoke contains organic and inorganic compounds that cue the seed of many species to germinate under post-fire conditions[6,7]. Among the organic compounds are karrikins, a family of butenolides that comprises six known members. In samples of smoke water generated by burning straw, KAR_1 is the most abundant karrikin, followed by KAR_2[8]. These two analogues differ by the presence or absence, respectively, of a methyl group on the butenolide ring (Supplementary Fig. 1a).

Karrikin mode of action has been elucidated by studies using *Arabidopsis thaliana*, a weedy ephemeral widely distributed in temperate climates throughout the northern hemisphere. Although seed germination in *A. thaliana* is stimulated by karrikins[3], this species is not

46 specifically associated with fire-prone habitats. *A. thaliana* is unusual in that it responds
47 preferentially to KAR_2, whereas most karrikin-responsive species, including fire-followers,
48 respond preferentially to KAR_1[1,9]. To understand the molecular basis for differential
49 sensitivity to distinct karrikins, we chose to investigate a different member of the
50 Brassicaceae that responds preferentially to KAR_1.

51 *Brassica tournefortii* (Brassicaceae; sahara mustard) is an invasive weed native to the
52 Mediterranean and Middle East that blights many semi-arid areas in North America, Australia
53 and South Africa. Infestations with *B. tournefortii* lead to dramatic reductions in plant cover of
54 native annuals, which suffer reduced stem and flower production, especially after relatively
55 wet winters[10]. *B. tournefortii* seed can persist in the soil for many seasons, undergoing wet-
56 dry cycling that can influence dormancy and contribute to boom-bust cycles that outcompete
57 native species[11-13]. Semi-arid Mediterranean-type ecosystems are also prone to wildfires. As
58 an invasive species, *B. tournefortii* may radically alter fire frequency and intensity by
59 influencing fuel profiles[14,15], further exacerbating the impact of fire on susceptible native
60 ecosystems. In addition, *B. tournefortii* is particularly responsive to KAR_1 and shows a positive
61 germination response in the nanomolar range[16]. Accordingly, although *B. tournefortii* is not
62 dependent on fire to spread, it is particularly well positioned to invade areas disturbed by fire
63 events[17,18].

64 To characterise the karrikin response of *B. tournefortii*, we performed multiple physiological
65 and molecular assays comparing KAR_1 with KAR_2. First, germination of *B. tournefortii* seeds
66 was consistently more sensitive to KAR_1 than KAR_2 at 10 nM, 100 nM and 1 μM (Fig. 1a and
67 Supplementary Fig. 1b-d). Second, expression of two karrikin-responsive genes, *BtDLK2* and
68 *BtSTH7*, required ten-fold higher concentrations of KAR_2 (1 μM) compared with KAR_1 (100
69 nM) for equivalent responses (Fig. 1b). Third, we found that KAI2 protein in *B. tournefortii*
70 (BtKAI2) degraded upon karrikin treatment, as is the case for *Arabidopsis* KAI2 (AtKAI2)[19].
71 Degradation of BtKAI2 in *B. tournefortii* seed was approximately 10-fold more sensitive to
72 KAR_1 than to KAR_2, such that after 48 h and 72 h treatment, 100 nM KAR_1 and 1 μM KAR_2
73 induced similar levels of KAI2 degradation (Fig. 1c). To rule out differential karrikin uptake to
74 account for these differences, we tested the absorption of KAR_1 and KAR_2 and found that both
75 were taken up at similar rates from solution by seeds during imbibition (Supplementary Fig.
76 1e-f). Besides promoting germination of primary dormant seeds, karrikins also inhibited
77 hypocotyl elongation in *B. tournefortii* seedlings, as is the case in *Arabidopsis*; again, KAR_1
78 showed a stronger effect than KAR_2, most clearly at 1 μM (Fig. 1d). Therefore, we conclude

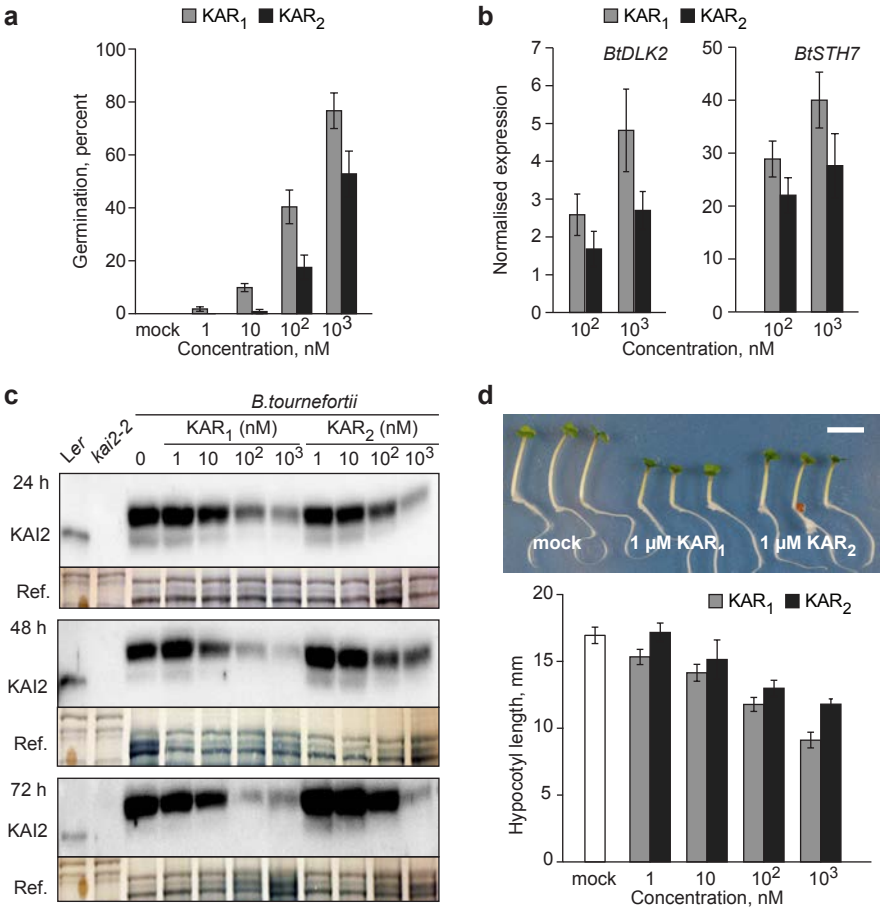

Figure 1: B. *tournefortii* is highly sensitive to KAR_1, the major karrikin analogue isolated from smoke
a, Germination responses of *B. tournefortii* seed to KAR_1 and KAR_2. Data are means ± SE; *n* = 3 biological replicates per treatment, ≥35 seeds per replicate. **b**, Levels of karrikin-responsive transcripts *BtDLK2* and *BtSTH7* in *B. tournefortii* seed. Seed were imbibed for 24 hours in the dark supplemented with KAR_1 and KAR_2. Transcripts were normalised to *BtCACS* reference transcripts. Data are means ± SE, *n* = 3 biological replicates, ≥50 seeds per replicate. **c**, Degradation of BtKAI2 protein levels in *B. tournefortii* seeds treated with KAR_1 and KAR_2 for 24, 48, and 72 hours. For each sample, 30 µg total protein isolated from imbibed seeds was separated by SDS-PAGE, blotted, and challenged with anti-KAI2 antibody. The reference panel shows the blot stained by amido black. Samples from *A. thaliana* ecotype L*er* and *kai2-2* seedlings serve as controls for antibody specificity. **d**, Hypocotyl elongation responses of *B. tournefortii* seedlings treated with KAR_1 and KAR_2. Data are means ± SE of *n* = 3 biological replicates, ≥12 seedlings per replicate. Scale bar: 10 mm.

79 that *B. tournefortii* is more sensitive to KAR_1 than to KAR_2. This pattern of ligand preference is
80 true of many karrikin-responsive species from ecosystems prone to wildfires[1,9], but notably is
81 opposite to that of *Arabidopsis*[3,4].

82 Orthologues of *KARRIKIN INSENSITIVE2/HYPOSENSITIVE TO LIGHT* (*KAI2/HTL*) are
83 ubiquitous in land plants, and are normally present as a single gene copy within an ancient
84 and highly conserved "eu-KAI2" clade[20]. There is growing evidence that, beyond its ability to
85 mediate karrikin responses, KAI2 has a core ancestral role in perceiving an endogenous
86 karrikin-like ligand ("KL") that regulates seed germination, seedling development, leaf shape
87 and cuticle development[21-23]. The genus *Brassica* has undergone a whole genome triplication
88 event since its divergence from the Arabidopsis lineage[24-26]. This process might have allowed
89 additional KAI2 copies to gain altered substrate specificity, potentially enhancing perception
90 of environmental signals such as karrikins from smoke.

91 To establish whether there are multiple *KAI2* homologues present in *B. tournefortii*, we
92 examined transcriptomes from seeds and seedlings. Three putative *KAI2* homologues were
93 identified (*BtKAI2a*, *BtKAI2b*, and *BtKAI2c*; Fig. 2a; Supplementary Fig. 2 and 3). *BtKAI2a*
94 grouped with *AtKAI2* and those of other Brassicaceae within a single clade, whereas *BtKAI2b*
95 and *BtKAI2c* grouped within a clade unique to *Brassica*. This phylogenetic pattern implies that
96 *BtKAI2a* is the ancestral copy of *KAI2*, whereas *BtKAI2b* and *BtKAI2c* arose more recently via
97 genome triplication within *Brassica*. All three *BtKAI2* transcripts were expressed in *B.*
98 *tournefortii* seeds, but only *BtKAI2a* and *BtKAI2b* could be detected in seedlings (Fig. 2b). In
99 both tissues, *BtKAI2b* transcripts were the most abundantly expressed of the three. We also
100 identified two *BtD14* homologues, at least one of which is functionally orthologous to *AtD14*
101 (Supplementary Figs. 2 and 4).

102 We performed transgenic complementation of the *Arabidopsis kai2-2* null mutant by
103 expressing each of the three isoforms as a GFP fusion protein driven by the *Arabidopsis KAI2*
104 promoter (*KAI2pro*:*GFP-BtKAI2*). Such fusions of GFP with KAI2 proteins have been used
105 previously with to analyse KAI2 activity[19,27,28]. Both *BtKAI2a* and *BtKAI2b* complemented the
106 seedling and leaf phenotypes of *kai2-2*, whereas *BtKAI2c* did not, despite being expressed at
107 the transcriptional level (Fig. 2c,d and Supplementary Fig. 5c). We could not detect GFP-
108 BtKAI2c protein in three independent transgenic lines, while GFP-BtKAI2a and GFP-BtKAI2b
109 accumulated at consistent levels (Fig. 2e). Following transient expression in tobacco leaves,
110 levels of BtKAI2c protein were considerably lower than for BtKAI2a and BtKAI2b, suggesting

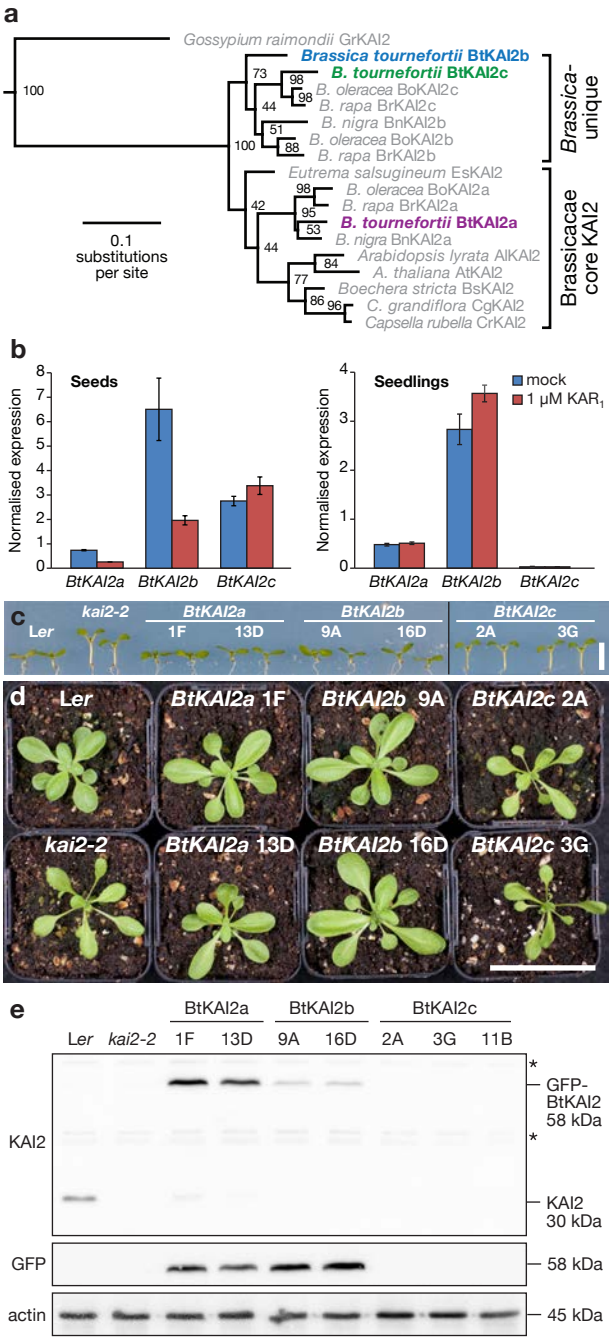

Figure 2 Two differentially expressed *B. tournefortii* KAI2 homologues are functional in Arabidopsis
a, Maximum likelihood phylogeny of KAI2 homologues in the Brassicaceae, based on nucleotide data. Node values represent bootstrap support from 100 replicates. A *KAI2* sequence from *Gossypium raimondii* (Malvaceae) serves as an outgroup. Tree shown is a subset of a larger phylogeny in Supplementary Figure 2. **b**, Transcript levels of the three *BtKAI2* homologues in seed imbibed for 24 h (left) and four-day-old seedlings treated with or without 1 μM KAR_1 for 24 h. **c, d,** Seedling and rosette phenotypes of two independent transgenic lines of Arabidopsis homozygous for *KAI2pro:GFP-BtKAI2x* transgenes. **e**, Immunoblots of soluble proteins challenged with antibodies against KAI2 (upper panel), GFP (middle panel) or actin (lower panel). Non-specific bands are marked with asterisks. Protein was isolated from pools of approximately fifty 7-day-old seedlings.

111 that BtKAI2c may be poorly expressed in plant cells (Supplementary Fig. 5b). BtKAI2c carries
112 several unique amino acid substitutions, which together may compromise protein folding and
113 stability (Supplementary Fig. 3). Therefore, we conclude that BtKAI2a and BtKAI2b are
114 functionally orthologous to AtKAI2 in regulating plant development, whereas BtKAI2c is non-
115 functional and may constitute a pseudogene.

116 We further characterised the ligand preference of *BtKAI2* homologues by performing
117 physiological and molecular assays with the transgenic lines. Primary-dormant Arabidopsis
118 seeds homozygous for the transgenes were tested for germination response. Germination of
119 *BtKAI2b* transgenic seeds was more responsive to KAR_1 than KAR_2 at 1 μM, whereas no
120 significant difference was observed for *BtKAI2a* transgenic seeds (Fig. 3a and Supplementary
121 Fig. 6). *BtKAI2c* transgenic seeds were insensitive to karrikins. Hypocotyl elongation
122 responses (Fig. 3b) and accumulation patterns of *DLK2* transcripts (Fig. 3c) agreed with the
123 germination response with respect to karrikin preferences. Therefore, and consistent with
124 their relative phylogenetic positions (Fig. 2a), we conclude that *BtKAI2a* has similarity to
125 *AtKAI2* in terms of ligand preference, whereas *BtKAI2b* has a preference for KAR_1 over KAR_2.
126 As *BtKAI2b* is more highly expressed than *BtKAI2a* in *B. tournefortii* seed and seedlings, we
127 suggest that the ligand preference of BtKAI2b accounts for the enhanced KAR_1-
128 responsiveness of this species.

129 To investigate the ligand preferences of BtKAI2a and BtKAI2b in more detail, we performed
130 differential scanning fluorimetry (DSF) assays on purified recombinant proteins. DSF has
131 been used extensively for inferring the interaction of strigolactone-like compounds with D14-
132 and KAI2-related proteins[28-32]. Racemic GR24 is a widely-used synthetic strigolactone
133 analogue that consists of two enantiomers, of which $GR24^{ent\text{-}5DS}$ is bioactive via AtKAI2[33].
134 Catalytically inactive D14 and KAI2 variants do not respond to GR24 in DSF, suggesting that
135 the shift in thermal response results from ligand hydrolysis and a corresponding
136 conformational change in the receptor[28-30]. In DSF assays, AtKAI2 shows a specific response to
137 >100 μM $GR24^{ent\text{-}5DS}$ but, for unclear reasons, no response at all to karrikins[28]. Likewise, we
138 found that both BtKAI2a and BtKAI2b were also unresponsive to karrikins in DSF
139 (Supplementary Fig. 7a). Therefore, we used $GR24^{ent\text{-}5DS}$ as a surrogate substrate in DSF
140 assays to infer BtKAI2–ligand interactions. We found that AtKAI2 and BtKAI2a showed similar
141 responses to >100 μM $GR24^{ent\text{-}5DS}$, but the BtKAI2b response was clear at >25 μM
142 (Supplementary Fig. 7b). We then used a lower range of $GR24^{ent\text{-}5DS}$ concentrations (0–50 μM)
143 to determine the threshold for response, which we defined as a statistically significant

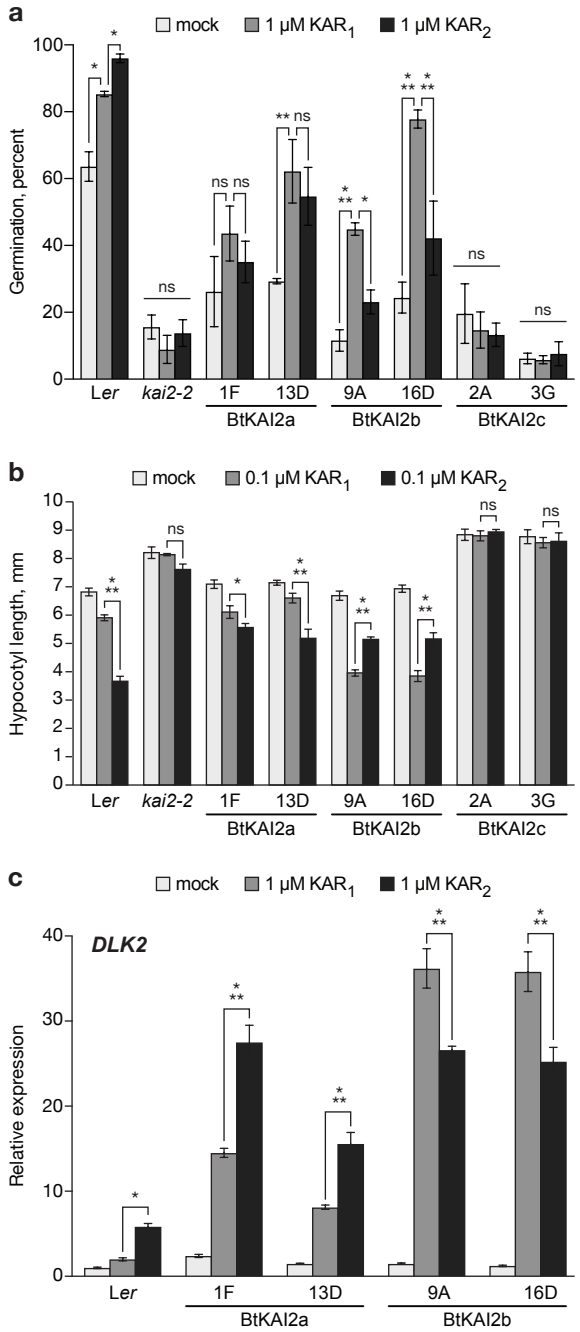

Figure 3. Functional divergence between BtKAI2 homologues

a, Germination responses of primary dormant Arabidopsis seed homozygous for *KAI2pro:GFP-BtKAI2* transgenes in the *kai2-2* background. Germination values were determined 120 h after sowing. Extended germination curves are shown in Supplementary Fig. 6. Data are means ± SE of n = 3 independent seed batches, 75 seed per batch. **b**, Hypocotyl elongation responses of *KAI2pro:GFP-BtKAI2x* seedlings treated with KAR_1 or KAR_2. Data are means ± SE of n = 3 biological replicates, 12–18 seedlings per replicate. **c**, Levels of *DLK2* transcripts in 8-day-old *KAI2pro:GFP-BtKAI2x* seedlings treated with KAR_1 or KAR_2 for eight hours. Expression was normalised to *CACS* reference transcripts and scaled to the value for mock-treated seedlings within each genotype. Data are means ± SE of n = 3 biological replicates. Pairwise significant differences: * $P < 0.05$ ** $P < 0.01$ *** $P < 0.001$; ns, $P > 0.05$ (ANOVA).

144 reduction in the maximal rate of change in fluorescence at the melting temperature of the
145 protein (T_m). Although BtKAI2a showed only a weak and non-significant response at 40 and
146 50 μM GR24$^{ent\text{-}5DS}$, BtKAI2b responded significantly at 10 μM and above (Fig. 4a). These
147 results suggest that BtKAI2b is more sensitive than BtKAI2a to GR24$^{ent\text{-}5DS}$, and that BtKAI2a is
148 most like AtKAI2 in this respect.

149 BtKAI2a and BtKAI2b differ in primary amino acid sequence at just 14 positions
150 (Supplementary Fig. 4). We postulated that differences in ligand preference might be
151 determined by amino acids in the vicinity of the ligand binding pocket. Protein structural
152 homology models revealed only two residues that differ in this region: V98 and V191 in
153 BtKAI2a, and L98 and L191 in BtKAI2b; the corresponding residues in AtKAI2 are V96 and
154 V189 (Fig. 4b-d). Residue 98 is immediately adjacent to the catalytic serine at the base of the
155 pocket. Residue 191 is located internally on αT4 of the lid domain which, in AtD14, is
156 associated with a major rearrangement of protein structure upon ligand binding that reduces
157 the size of the pocket[34]. Homology modelling suggests only subtle differences in the size and
158 shape of the primary ligand binding pocket of BtKAI2a and BtKAI2b (Fig. 4b-d), but L98
159 would make the BtKAI2b pocket more hydrophobic, which is consistent with KAR_1 being
160 more hydrophobic than KAR_2[8]. To determine if these residues are pertinent to ligand
161 response, we replaced the two valine residues of BtKAI2a with leucine residues, generating
162 the variant BtKAI2a(b), and vice-versa for BtKAI2b, generating the variant BtKAI2b(a). In DSF
163 assays, we found that exchanging the two residues was sufficient to switch the original
164 responses, such that BtKAI2a(b) responded sensitively to GR24$^{ent\text{-}5DS}$, but BtKAI2b(a) did not
165 (Fig. 4e). Finally, to validate the different effects observed with GR24$^{ent\text{-}5DS}$ upon BtKAI2a and
166 BtKAI2b *in vitro*, we examined the response of these proteins to GR24$^{ent\text{-}5DS}$ *in planta*. We
167 found that, in terms of induction of *DLK2* transcripts, *GFP-BtKAI2b* transgenic seedlings
168 responded more strongly than *GFP-BtKAI2a* and wild type L*er* seedlings to 0.1 μM GR24$^{ent\text{-}5DS}$
169 (Fig. 4f). Overall, these results suggest that two variant residues can account for differences in
170 substrate preference between BtKAI2a and BtKAI2b. Given the importance of these residues,
171 it is notable that the non-functional BtKAI2c carries a highly non-conservative Leu-to-Arg
172 substitution at position 98 (Supplementary Fig. 3).

173 Two crystal structures of KAI2 proteins from *Arabidopsis thaliana* and *Striga hermonthica* are
174 non-congruent with respect to KAR_1 binding position and orientation[5,35]. In addition, the
175 affinity of AtKAI2 for KAR_1 is poorly defined, with estimates of dissociation coefficients (Kd)
176 ranging from 4.6 μM[36] to 148 μM[37] using isothermal calorimetry; for comparison, the Kd value

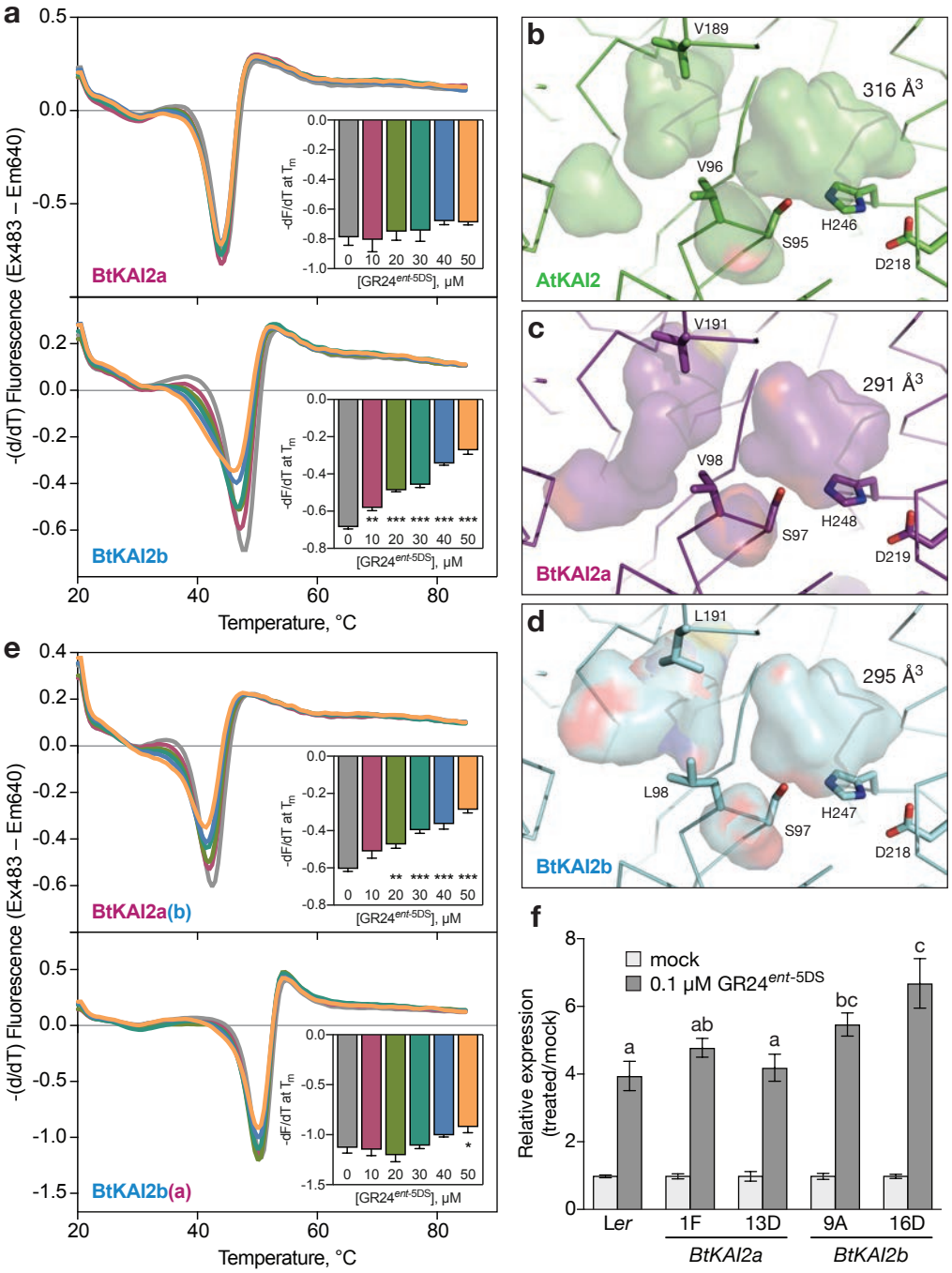

Figure 4. Two residues account for ligand specificity between BtKAI2a and BtKAI2b
a, DSF curves of SUMO-BtKAI2a and SUMO-BtKAI2b fusion proteins treated with 0-50 µM GR24$^{ent\text{-}5DS}$, a KAI2-bioactive ligand. Each curve is the average of three sets of reactions, each comprising four technical replicates. Insets plot the minimum value of –(dF/dT) at the melting point of the protein as determined in the absence of ligand (means ± SE, n = 3). Significant differences from untreated control: * $P < 0.05$ ** $P < 0.01$ *** $P < 0.001$ (ANOVA). **b–d**, Solved structure of AtKAI2 (PDB: 3w06, Kagiyama et al 2013) (b) and derived homology models (c–d) of BtKAI2a and BtKAI2b. Coloured surfaces depict internal cavities; values indicate the volumes of the primary ligand-binding cavities, adjacent to the catalytic Ser-His-Asp residues. Also shown is a variable secondary pocket, to the left of the primary pocket in these images. **e**, DSF curves of SUMO-BtKAI2a(b) and SUMO-BtKAI2b(a) fusion proteins treated with 0-50 µM GR24$^{ent\text{-}5DS}$. **f**, Levels of *DLK2* transcripts (normalized to *CACS* reference transcripts) in two independent lines of *KAI2pro:GFP-BtKAI2a* and *-BtKAI2b* seedlings treated for two hours with 0.1 µM GR24$^{ent\text{-}5DS}$. Data are means ± SE; n = 3 biological replicates. Letters indicate significantly different groupings (ANOVA; P < 0.05).

177 of AtD14 for GR24 is 0.3 μM using the same technique[36]. As such, it has been difficult to
178 establish a definitive receptor-ligand relationship for KAI2 and karrikins. Our results provide
179 strong evidence that KAI2 has the capacity to confer karrikin specificity, which in turn
180 demonstrates that KAI2 is the receptor for karrikins. However, we cannot rule out the
181 possibility that karrikins interact with the receptor differently from GR24$^{ent\text{-}5DS}$, which may
182 account for the inactivity of karrikins in DSF assays.

183 The ligand binding pocket of KAI2 is generally hydrophobic, but the key residues that confer
184 ligand specificity are not clear. In certain root-parasitic weeds in the Orobanchaceae,
185 substitutions of bulky residues found in AtKAI2 with smaller hydrophobic amino acids have
186 potentially improved the affinity for host-derived strigolactone ligands with different
187 structural configurations[38,39]. In the case of BtKAI2 proteins, the more subtle changes in
188 pocket residues likely account for fine-tuning between very similar ligands. Similarly subtle
189 changes have been reported for the rice gibberellin receptor GID1: changing Ile133 to Leu or
190 Val increases the affinity for GA_{34} relative to GA_4, which differ by just one hydroxyl group[40].

191 Gene duplication is a common feature in plant evolutionary histories that can allow genes to
192 acquire new functions[41]. In obligate parasitic weeds, duplication and diversification of
193 *KAI2*/*HTL* genes have shifted ligand specificity towards strigolactones. Crucially, the core
194 KAI2 function of perceiving an endogenous ligand ("KL") is presumably retained through
195 ancestral, non-divergent copies that are under purifying selection[38,39]. KAI2 diversity may also
196 reflect differing affinity for KL in different species and at different life stages. Our results are
197 consistent with a scenario in which both BtKAI2a and BtKAI2b have retained the core KAI2
198 function of perceiving KL to support plant development. However, BtKAI2b has also acquired
199 mutations that alter its substrate specificity, which in turn enhance sensitivity to the more
200 abundant karrikin released after fire. This diversity among KAI2 proteins potentially provides
201 *B. tournefortii* with a selective advantage in fire-prone environments, assisting its invasive
202 nature.

203 Recent findings indicate that KAI2 is an integrator that also modulates germination in
204 response to abiotic environmental signals, including temperature and salinity[42]. As seed
205 germination is a critical life stage that contributes to the invasiveness of a species, strategies
206 for weed control will benefit from specific knowledge of KAI2 sequence diversity and
207 expression profiles.

208 # METHODS

209 ## Chemical synthesis

210 Karrikins (KAR_1 and KAR_2), $^{13}[C]_5$-labelled karrikins and GR24 enantiomers ($GR24^{5DS}$ and
211 $GR24^{ent\text{-}5DS}$) were prepared as previously described[1,9,43-45].

212 ## Plant material

213 Arabidopsis *kai2-2* (L*er*) and *Atd14-1* (Col-0) mutants were previously described[4]. The seeds
214 of *Brassica tournefortii* used in this work were collected in November and December 2009
215 from two sites in Western Australia (Kings Park in Perth, and Merridin) as described
216 previously[46]. Seeds were dried to 15% relative humidity for one month prior to storage in air-
217 tight bags at –20 °C.

218 ## Seed germination assays

219 Seed germination assays using Arabidopsis were performed on Phytagel as described
220 previously[33]. *Brassica tournefortii* seeds were sowed in triplicates (35-70 seeds each) on glass
221 microfibre filter paper (Grade 393; Filtech, NSW Australia) held in petri dishes and
222 supplemented with mock or karrikin treatments. Treatments were prepared by diluting
223 acetone (mock) or karrikin stocks (dissolved in acetone) 1:1000 with ultrapure water. The
224 seeds were imbibed in the dark at 22 °C. Numbers of germinated seeds were counted each day
225 until the germination percentages remained unchanged.

226 ## Hypocotyl elongation assays

227 Arabidopsis hypocotyl elongation assays were performed under red light as described
228 previously[4]. For *B. tournefortii*, assays were performed with the following modifications to the
229 Arabidopsis protocol: *B. tournefortii* seeds were sowed in triplicate on glass microfibre filter
230 paper (Filtech) held in petri-dishes supplemented with mock or karrikin treatments. The
231 seeds were imbibed in the dark for 22 h at 22 °C before exposing to continuous red light (20
232 µmol photons m^{-2} s^{-1}) for 3 days.

233 ## KAI2 degradation assays

234 *B. tournefortii* seeds were imbibed on glass fibre filters as described above and incubated in
235 the dark at 22°C. Imbibition solutions contained the indicated concentration of karrikins.

236 Seeds were harvested after 24, 48 and 72 h and frozen in liquid nitrogen. Protein extraction
237 and immunoblotting were conducted as previously described[28]. The reference panels show a
238 representative region of each blot stained with amido black solution (0.03% w/v in 1:10
239 acetic acid:methanol).

240 **Transcript analysis**

241 *Brassica tournefortii* seeds were imbibed on glass fibre filters in the dark at 22 °C as described
242 above For transcript quantification in *B. tournefortii* seeds, samples were taken at the
243 indicated time points, briefly blot-dried on paper towel, and frozen in liquid nitrogen. For *B.*
244 *tournefortii* seedlings, seeds imbibed for 24 h were transferred to the growth room (~120-
245 150 µmol photons m^{-2} s^{-2}, 16 h light/8 h dark, 22 °C light/16 °C dark) for three days. A sample
246 of approximately 20 seedlings was then transferred to a 250 mL conical flask containing 50
247 mL ultrapure water supplemented with 1 µM KAR_1, or an equivalent volume of acetone (0.1%
248 v/v), with three replicate samples per treatment. The flasks were then shaken for 24 h before
249 seedlings were harvested.

250 Arabidopsis seedlings were grown on 0.5× MS agar under the same growth room conditions
251 for seven days. On the seventh day, seedlings were transferred to 3 mL liquid 0.5× MS
252 medium in 12-well culture plates (CORNING Costar 3513) and shaken at 70 rpm for a further
253 22 h. The medium was then removed by pipette and replaced with fresh medium containing
254 relevant compounds or an equivalent volume (0.1% v/v) acetone. After a further incubation
255 period with shaking (between 2 and 8 h), the seedlings were harvested, blotted dry, and
256 frozen in liquid nitrogen.

257 RNA extraction, DNase treatment, cDNA synthesis and quantitative PCR were conducted as
258 previously described [47]. Oligonucleotides are listed in the Supplementary Table 2.

259 **Cloning and mutagenesis of *Brassica tournefortii KAI2* and *D14* homologues**

260 The Gateway-compatible destination vector pMDC43[48] was digested with *Hind*III and *Kpn*I to
261 release the 35S promoter, which was replaced with the 776-bp *KAI2* promoter and 5′UTR as
262 defined previously [28], yielding the binary destination vector pKAI2pro-GFP-GW. Due to high
263 sequence similarity among BtKAI2 and BtD14 paralogues in the coding region, unique
264 transcripts were identified on the basis of distinct 3′UTRs. Full-length *BtKAI2* coding
265 sequences (and unique 3′UTR sequences) were amplified from *B. tournefortii* cDNA with the
266 *attB* sites using the universal forward primer BtKAI2_universal_F and homologue-specific

267 reverse primers RACE_R (BtKAI2a), Contig1_R (BtKAI2b) and Contig5_R (BtKAI2c), before
268 cloning into pDONR207 (Life Technologies). The pDONR207 clones were confirmed by Sanger
269 sequencing and recombined with pKAI2pro-GFP-GW to generate the binary plant expression
270 plasmids pKAI2pro-GFP-BtKAI2a, pKAI2pro-GFP-BtKAI2b and pKAI2pro-GFP-BtKAI2c. For
271 transient expression in tobacco, BtKAI2 coding sequences were transferred via Gateway-
272 mediated recombination into pSKI106, which drives very high expression and encodes an N-
273 terminal 3× *c*-myc tag[49]. The *BtD14a* coding sequence was amplified from cDNA using
274 oligonucleotides BtD14_F and BtD14_R, cloned into pDONR207 as above, and transferred into
275 pD14pro-GW [28].

276 The full-length *BtKAI2* coding sequences (excluding 3′UTR) were amplified from the
277 pDONR207 clones and reconstituted with the pE-SUMO vector by Gibson Assembly to
278 generate the heterologous expression plasmids pE-SUMO-BtKAI2a, pE-SUMO-BtKAI2b and
279 pE-SUMO-BtKAI2c. Site-directed mutagenesis was performed on pE-SUMO-BtKAI2a and pE-
280 SUMO-BtKAI2b clones to generate the heterologous expression plasmids pE-SUMO-
281 BtKAI2a(b) and pE-SUMO-BtKAI2b(a). Both targeted residues were mutated simultaneously
282 in one PCR product, while the remainder of the plasmid was amplified in a second PCR
283 product. The mutated plasmids were reconstituted by Gibson assembly, and coding regions
284 confirmed by Sanger sequencing.

285 **Plant transformation**

286 Homozygous *kai2-2* plants were transformed by floral dip. Primary transgenic seedlings were
287 selected on sterile 0.5× MS medium supplemented with 20 μg/mL hygromycin B. T_2 lines
288 exhibiting a 3:1 ratio of hygromycin resistant-to-sensitive seedlings were propagated further
289 to identify homozygous lines in the T_3 generation. Experiments were performed from the T_3
290 generation onwards.

291 For transient expression in tobacco, *Agrobacterium* (GV3101) carrying pSKI106 variants was
292 grown in LB medium (25 mL) supplemented with antibiotics and 20 μM acetosyringone until
293 OD_{600} reached 1.0. The bacteria were then harvested by centrifugation (15 min, 5000 × *g*) and
294 resuspended in 10 mM $MgCl_2$, 10 mM MES (pH 5.6) and 100 μM acetosyringone. The optical
295 density was adjusted to 0.4, and the suspension was left standing at 22 °C overnight
296 (approximately 14 h). Leaves of three-week-old *Nicotiana bethamiana* were then infiltrated
297 with a 5-mL syringe, through the abaxial leaf surface. After four days, the leaves were
298 collected and frozen in liquid nitrogen.

299 ## Karrikin uptake measurements

300 Fifteen samples of seed were sowed for each karrikin treatment (five time points, each in
301 triplicate). In each sample, approximately 40 mg of *Brassica tournefortii* seeds were imbibed
302 in 3 mL ultrapure water for 24 h in 5-mL tubes. After centrifugation (2 min at 3220 × *g*),
303 excess water was removed by pipette and the volume of residual water (mostly absorbed into
304 the seeds) was calculated by weighing the seeds before and after imbibition. Fresh ultrapure
305 water was added to the fully-imbibed seeds to reach a total volume of 980 µL. Then 20 µL of
306 100 µM KAR_1 or KAR_2 was added to a final concentration of 2 µM. The seeds were imbibed at
307 22 °C in darkness. At the indicated time point (0, 2, 4, 8 or 24 h post-treatment), 500 µL of the
308 imbibition solution was removed and combined with 100 ng of either $^{13}[C]_5$-KAR_1 or $^{13}[C]_5$-
309 KAR_2 (100 µL at 1 µg/mL) as an internal standard for quantification purposes. The sample
310 was then extracted once with ethyl acetate (500 µL), and 1 µL of this organic layer was
311 analysed using GC-MS in selective ion monitoring (SIM) mode as previously described[50].

312 The amount of KAR_1 in each sample was calculated by the formula $\frac{A(Ion150)}{A(Ion155)}$×100 ng and
313 converted to moles, where *A(Ion150)* indicates the peak area of the ion 150 (KAR_1 to be
314 measured), *A(Ion151)* indicates the peak area of the ion 151 ($^{13}[C]_5$-KAR_1), and 100 ng is the
315 amount of $^{13}[C]_5$-KAR_1 spiked in before the ethyl acetate extraction. Similarly, the amount of
316 KAR_2 in each sample was calculated by the formula $\frac{A(Ion136)}{A(Ion141)}$×100 ng and converted to moles.

317 The uptake percentage adjusted to 40 mg of *B. tournefortii* seeds was calculated by the
318 formula: $(1 - \frac{N(x)}{N(0)}) \times \frac{40\ mg}{m\ (seed)}$, where N(0) indicates moles of karrikins at time 0, $N(x)$ indicates
319 moles of karrikins at time point *x*, and $m(seed)$ indicates the dry weight (mg) of seeds tested in
320 each replicate.

321 For Arabidopsis seeds, the procedure was scaled down for a smaller mass of seeds (20 mg).

322 ## Transcriptome assembly and analysis

323 Twenty milligrams of dry *B. tournefortii* seed was imbibed in water for 24 h and incubated at
324 22 °C in the dark. The seeds were collected by centrifugation, blotted dry, and frozen in liquid
325 nitrogen. A separate sample of seed was sown on glass filter paper, imbibed for 24 h as above,
326 and then incubated for 96 h under continuous red light (20 µmol m^{-2} s^{-1}) with a 22 °C (16
327 h)/16 °C (8h) temperature cycle. A single sample of seedlings (50 mg fresh weight) was

328 harvested and frozen in liquid nitrogen. Total RNA was extracted from both seed and seedling
329 samples using the Spectrum Plant RNA kit (Sigma-Aldrich), including an on-column DNase
330 step. PolyA$^+$ mRNA was purified using oligo(dT) magnetic beads (Illumina), and cDNA
331 libraries for sequencing were generated as described[51]. Sequencing was performed on the
332 Illumina HiSeq 2000 platform at the Beijing Genomic Institute, Shenzhen, China. Raw reads
333 were filtered to remove adapters and low quality reads (those with >5% unknown
334 nucleotides, or those in which greater than 20% of base calls had quality scores ≤10). After
335 filtering, both libraries generated reads with >99.9% of nucleotides attaining Q20 quality
336 score. Transcriptome *de novo* assembly was performed with Trinity[52]. For each library,
337 contigs were assembled into Unigenes; Unigenes from both libraries were then combined,
338 yielding a total of 45,553 predicted coding region sequences with a mean length of 1011 nt.
339 The combined Unigenes were then interrogated for homology to AtKAI2 and AtD14 using
340 BLASTn searches.

341 **Phylogenetic analysis**

342 *KAI2* and *D14* homologues in *Brassica* species were identified from BLAST searches using
343 Arabidopsis coding sequences as a query. Additional sequences were sampled from an
344 extended phylogenetic analysis[20]. Multiple sequence alignments were performed using
345 MAFFT plugin implemented in Geneious R10 (Biomatters). The alignment was trimmed
346 slightly at the 5′ end to remove non-aligned regions of monocot D14 sequences. Maximum
347 likelihood phylogenies were generated using PHYML (GTR +G +I substitution model,
348 combination of NNI and SPR search, and 100 bootstraps). The choice of substitution model
349 was guided by Smart Model Selection in PhyML (http://www.atgc-montpellier.fr/sms; [53]). A
350 list of all sequences, and their sources, is provided in Supplementary Table 1.

351 **Protein homology modelling**

352 KAI2 structures were modelled using the SWISS-MODEL server
353 (https://swissmodel.expasy.org) using the alignment mode[54] and the *Arabidopsis thaliana*
354 KAI2 structure 3w06 as a template[36]. Figures of protein structure and homology models were
355 generated using PyMOL v1.3 (Schrödinger LLC). Cavity surfaces were visualised using the
356 "cavities & pockets (culled)" setting in PyMOL and a cavity detection cut-off value of four
357 solvent radii. Cavity volumes were calculated using the CASTp server v3.0[55]
358 (http://sts.bioe.uic.edu/castp) with a probe radius of 1.4Å. Values indicate Connolly's solvent-
359 excluded volumes. Cavities were inspected visually using Chimera v1.12

360 (https://www.cgl.ucsf.edu/chimera/). For both BtKAI2a and BtKAI2b models, CASTp
361 erroneously included surface residues near the primary pocket entrance in the calculation of
362 the pocket volumes. This issue was resolved by the artificial placement of a free alanine
363 residue adjacent to the cavity entrance, as described previously[56].

364 ### Protein expression and purification

365 BtKAI2 proteins were generated as N-terminal 6×HIS-SUMO fusion proteins. All proteins were
366 expressed in BL21 Rosetta DE3 pLysS cells (Novagen) and purified using IMAC as described
367 previously[28].

368 ### Differential scanning fluorimetry

369 DSF was performed and thermal shifts were quantified as described previously[28]. Reactions
370 (10 µL) contained 20 µM protein, 20 mM HEPES pH 7.5, 150 mM NaCl, 1.25% (v/v) glycerol,
371 5× SYPRO Tangerine dye (Molecular Probes) and varying concentrations of ligand that
372 resulted in a final concentration of 5% (v/v) acetone.

373 ### Statistical analysis

374 Data were analysed using one- or two-way ANOVA (α = 0.05, with Holm-Sidak's multiple
375 comparisons test). Germination data were arcsin transformed prior to ANOVA. Tests were
376 implemented in GraphPad Prism version 7.0 (GraphPad Software, graphpad.com).

377 ### Sequence data

378 Sequence data are available at NCBI Genbank under the following accessions: *BtKAI2a*,
379 MG783328; *BtKAI2b*, MG783329; *BtKAI2c*, MG783330; *BtD14a*, MG783331; *BtD14b*,
380 MG783332; *BtDLK2*, MG783333. Raw RNA sequence data from *Brassica tournefortii* seed and
381 seedlings are available in the NCBI SRA database under accession SRP128835.

382 ## REFERENCES

383 1. Flematti, G. R., Ghisalberti, E. L., Dixon, K. W. & Trengove, R. D. A compound from smoke
384 that promotes seed germination. *Science* **305,** 977 (2004).
385 2. Nelson, D. C., Flematti, G. R., Ghisalberti, E. L., Dixon, K. W. & Smith, S. M. Regulation of
386 seed germination and seedling growth by chemical signals from burning vegetation.
387 *Ann Rev Plant Biol* **63,** 107–130 (2012).
388 3. Nelson, D. C. *et al.* Karrikins discovered in smoke trigger Arabidopsis seed germination

389 by a mechanism requiring gibberellic acid synthesis and light. *Plant Physiol* **149,** 863–
390 873 (2009).
391 4. Waters, M. T. *et al.* Specialisation within the DWARF14 protein family confers distinct
392 responses to karrikins and strigolactones in Arabidopsis. *Development* **139,** 1285–1295
393 (2012).
394 5. Guo, Y., Zheng, Z., La Clair, J. J., Chory, J. & Noel, J. P. Smoke-derived karrikin perception
395 by the α/β-hydrolase KAI2 from Arabidopsis. *Proc Natl Acad Sci USA* **110,** 8284–8289
396 (2013).
397 6. Flematti, G. R. *et al.* Karrikin and Cyanohydrin Smoke Signals Provide Clues to New
398 Endogenous Plant Signaling Compounds. *Mol Plant* **6,** 29–37 (2013).
399 7. Keeley, J. E. & Pausas, J. G. Evolution of 'smoke' induced seed germination in
400 pyroendemic plants. *South African Journal of Botany* **115,** 251–255 (2018).
401 8. Flematti, G. R., Ghisalberti, E. L., Dixon, K. W. & Trengove, R. D. Identification of Alkyl
402 Substituted 2 H-Furo[2,3- c]pyran-2-ones as Germination Stimulants Present in Smoke.
403 *J Agric Food Chem* **57,** 9475–9480 (2009).
404 9. Flematti, G. R. *et al.* Preparation of 2H-furo[2,3-c]pyran-2-one derivatives and
405 evaluation of their germination-promoting activity. *J Agric Food Chem* **55,** 2189–2194
406 (2007).
407 10. Barrows, C. W., Allen, E. B., Brooks, M. L. & Allen, M. F. Effects of an invasive plant on a
408 desert sand dune landscape. *Biol Invasions* **11,** 673–686 (2009).
409 11. Bangle, D. N., Walker, L. R. & Powell, E. A. Seed germination of the invasive plant
410 *Brassica tournefortii* (Sahara mustard) in the Mojave Desert. *Western North American*
411 *Naturalist* **68,** 334–342 (2008).
412 12. Long, R. L. *et al.* Prior hydration of Brassica tournefortii seeds reduces the stimulatory
413 effect of karrikinolide on germination and increases seed sensitivity to abscisic acid.
414 *Ann Bot* **105,** 1063–1070 (2010).
415 13. Long, R. L. *et al.* Seeds of Brassicaceae weeds have an inherent or inducible response to
416 the germination stimulant karrikinolide. *Ann Bot* **108,** 933–944 (2011).
417 14. Brooks, M. L. *et al.* Effects of Invasive Alien Plants on Fire Regimes. *BioScience* **54,** 677
418 (2004).
419 15. Sanders, R. & Minnich, R. in *Invasive Plants of California's Wildlands* (eds. Bossard, C. C.,
420 Randall, J. M. & Hoshovsky, M. C.) 360 (University of California Press, 2000). at
421 <http://www.cal-ipc.org/resources/library/booksandcds/ipcw/online/>
422 16. Stevens, J., Merritt, D., Flematti, G., Ghisalberti, E. & Dixon, K. Seed germination of
423 agricultural weeds is promoted by the butenolide 3-methyl-2H-furo[2,3-c]pyran-2-one
424 under laboratory and field conditions. *Plant Soil* **298,** 113–124 (2007).
425 17. Schiermeier, Q. Pall hangs over desert's future as alien weeds fuel wildfires. *Nature*
426 **435,** 724 (2005).
427 18. Steers, R. J. Invasive Plants, Fire Succession, and Restoration of Creosote Bush Scrub in
428 Southern California. 1–210 (UNIVERSITY OF CALIFORNIA RIVERSIDE, 2008).
429 19. Waters, M. T., Scaffidi, A., Flematti, G. & Smith, S. M. Substrate-Induced Degradation of
430 the α/β-Fold Hydrolase KARRIKIN INSENSITIVE2 Requires a Functional Catalytic Triad
431 but Is Independent of MAX2. *Mol Plant* **8,** 814–817 (2015).
432 20. Bythell-Douglas, R. *et al.* Evolution of strigolactone receptors by gradual neo-
433 functionalization of KAI2 paralogues. *BMC Biol* **15,** 52 (2017).
434 21. Conn, C. E. & Nelson, D. C. Evidence that KARRIKIN-INSENSITIVE2 (KAI2) Receptors
435 may Perceive an Unknown Signal that is not Karrikin or Strigolactone. *Frontiers in Plant*
436 *Science* **6,** 1219 (2015).
437 22. Sun, Y. K., Flematti, G. R., Smith, S. M. & Waters, M. T. Reporter Gene-Facilitated
438 Detection of Compounds in Arabidopsis Leaf Extracts that Activate the Karrikin
439 Signaling Pathway. *Frontiers in Plant Science* **7,** 1799 (2016).

440 23. Li, W. *et al.* The karrikin receptor KAI2 promotes drought resistance in Arabidopsis
441 thaliana. *PLoS Genet* **13,** e1007076 (2017).
442 24. Martin A Lysak, M. A. K. A. P. I. S. Chromosome triplication found across the tribe
443 Brassiceae. *Genome Res.* **15,** 516–525 (2005).
444 25. Wang, X. *et al.* The genome of the mesopolyploid crop species Brassica rapa. *Nat Genet*
445 **43,** 1035–1039 (2011).
446 26. Liu, S. *et al.* The Brassica oleracea genome reveals the asymmetrical evolution of
447 polyploid genomes. *Nat Comms* **5,** 3930 (2014).
448 27. Sun, X.-D. & Ni, M. HYPOSENSITIVE TO LIGHT, an Alpha/Beta Fold Protein, Acts
449 Downstream of ELONGATED HYPOCOTYL 5 to Regulate Seedling De-Etiolation. *Mol*
450 *Plant* **4,** 116–126 (2011).
451 28. Waters, M. T. *et al.* A Selaginella moellendorffii Ortholog of KARRIKIN INSENSITIVE2
452 Functions in Arabidopsis Development but Cannot Mediate Responses to Karrikins or
453 Strigolactones. *Plant Cell* **27,** 1925–1944 (2015).
454 29. Hamiaux, C. *et al.* DAD2 Is an α/β Hydrolase Likely to Be Involved in the Perception of
455 the Plant Branching Hormone, Strigolactone. *Curr Biol* **22,** 2032–2036 (2012).
456 30. Abe, S. *et al.* Carlactone is converted to carlactonoic acid by MAX1 in Arabidopsis and its
457 methyl ester can directly interact with AtD14 in vitro. *Proc Natl Acad Sci USA* **111,**
458 18084–18089 (2014).
459 31. Végh, A. *et al.* Comprehensive Analysis of DWARF14-LIKE2 (DLK2) Reveals Its
460 Functional Divergence from Strigolactone-Related Paralogs. *Frontiers in Plant Science* **8,**
461 (2017).
462 32. Hamiaux, C. *et al.* Inhibition of strigolactone receptors by N-phenylanthranilic acid
463 derivatives: structural and functional insights. *Journal of Biological Chemistry* (2018).
464 doi:10.1074/jbc.RA117.001154
465 33. Scaffidi, A. *et al.* Strigolactone hormones and their stereoisomers signal through two
466 related receptor proteins to induce different physiological responses in Arabidopsis.
467 *Plant Physiol* **165,** 1221–1232 (2014).
468 34. Yao, R. *et al.* DWARF14 is a non-canonical hormone receptor for strigolactone. *Nature*
469 **536,** 469–473 (2016).
470 35. Xu, Y. *et al.* Structural basis of unique ligand specificity of KAI2-like protein from
471 parasitic weed Striga hermonthica. *Sci. Rep.* **6,** 31386 (2016).
472 36. Kagiyama, M. *et al.* Structures of D14 and D14L in the strigolactone and karrikin
473 signaling pathways. *Genes Cells* **18,** 147–160 (2013).
474 37. Lee, I. *et al.* Functional Analysis of a Missense Allele of KARRIKIN-INSENSITIVE2 that
475 Impairs Ligand-Binding and Downstream Signaling in Arabidopsis thaliana. *Journal of*
476 *Experimental Botany* (2018). doi:10.1093/jxb/ery164
477 38. Conn, C. E. *et al.* Convergent evolution of strigolactone perception enabled host
478 detection in parasitic plants. *Science* **349,** 540–543 (2015).
479 39. Toh, S. *et al.* Structure-function analysis identifies highly sensitive strigolactone
480 receptors in Striga. *Science* **350,** 203–207 (2015).
481 40. Shimada, A. *et al.* Structural basis for gibberellin recognition by its receptor GID1.
482 *Nature* **456,** 520 (2008).
483 41. Panchy, N., Lehti-Shiu, M. D. & Shiu, S.-H. Evolution of gene duplication in plants. *Plant*
484 *Physiol* pp.00523.2016 (2016). doi:10.1104/pp.16.00523
485 42. Wang, L., Waters, M. T. & Smith, S. M. Karrikin-KAI2 signalling provides Arabidopsis
486 seeds with tolerance to abiotic stress and inhibits germination under conditions
487 unfavourable for seedling establishment. *New Phytol* (2018). doi:10.1111/nph.15192
488 43. Goddard-Borger, E. D., Ghisalberti, E. L. & Stick, R. V. Synthesis of the germination
489 stimulant 3-methyl-2H-furo[2,3-c]pyran-2-one and analogous compounds from
490 carbohydrates. *Eur J Org Chem* 3925–3934 (2007). doi:10.1002/ejoc.200700334

491 44. Mangnus, E., Dommerholt, F., Jong, R. de & Zwanenburg, B. Improved synthesis of strigol
492 analog GR24 and evaluation of the biological-activity of its diastereomers. *J Agric Food*
493 *Chem* **40,** 1230–1235 (1992).
494 45. Scaffidi, A. *et al.* The synthesis and biological evaluation of labelled karrikinolides for
495 the elucidation of the mode of action of the seed germination stimulant. *Tetrahedron*
496 **67,** 152–157 (2011).
497 46. Gorecki, M. J., Long, R. L., Flematti, G. R. & Stevens, J. C. Parental environment changes
498 the dormancy state and karrikinolide response of Brassica tournefortii seeds. *Ann Bot*
499 (2012). doi:10.1093/aob/mcs067
500 47. Waters, M. T. & Smith, S. M. KAI2- and MAX2-Mediated Responses to Karrikins and
501 Strigolactones Are Largely Independent of HY5 in Arabidopsis Seedlings. *Mol Plant* **6,**
502 63–75 (2013).
503 48. Curtis, M. D. & Grossniklaus, U. A gateway cloning vector set for high-throughput
504 functional analysis of genes in planta. *Plant Physiol* **133,** 462–469 (2003).
505 49. Kagale, S. *et al.* TMV-Gate vectors: gateway compatible tobacco mosaic virus based
506 expression vectors for functional analysis of proteins. *Sci. Rep.* **2,** 874 (2012).
507 50. Flematti, G. R., Scaffidi, A., Dixon, K. W., Smith, S. M. & Ghisalberti, E. L. Production of the
508 seed germination stimulant karrikinolide from combustion of simple carbohydrates. *J*
509 *Agric Food Chem* **59,** 1195–1198 (2011).
510 51. Liang, C., Liu, X., Yiu, S.-M. & Lim, B. L. De novo assembly and characterization of
511 Camelina sativa transcriptome by paired-end sequencing. *BMC Genomics 2013 14:1* **14,**
512 146 (2013).
513 52. Grabherr, M. G. *et al.* Full-length transcriptome assembly from RNA-Seq data without a
514 reference genome. *Nat Biotechnol* **29,** 644–652 (2011).
515 53. Lefort, V., Longueville, J.-E. & Gascuel, O. SMS: Smart Model Selection in PhyML. *Mol Biol*
516 *Evol* **34,** 2422–2424 (2017).
517 54. Bordoli, L. *et al.* Protein structure homology modeling using SWISS-MODEL workspace.
518 *Nat Protoc* **4,** 1–13 (2009).
519 55. Dundas, J. *et al.* CASTp: computed atlas of surface topography of proteins with
520 structural and topographical mapping of functionally annotated residues. *Nucleic Acids*
521 *Res* **34,** W116–W118 (2006).
522 56. Lopez-Obando, M. *et al.* Structural modelling and transcriptional responses highlight a
523 clade of PpKAI2-LIKE genes as candidate receptors for strigolactones in Physcomitrella
524 patens. *Planta* **243,** 1441–1453 (2016).
525

526 ## ACKNOWLEDGEMENTS

527 This work was supported by funding from the Australian Research Council (DP130103646
528 to SMS and GRF; DP140104567 to SMS; FT150100162 to MTW, DP160102888 to GRF and
529 MTW). Y.K.S was recipient of a Research Training Program Scholarship from the Australian
530 Government. We thank Dr Rowena Long for the original provision of *B. tournefortii* seeds, Dr
531 Rohan Bythell-Douglas for advice on homology modelling, and Mr Yongjie Meng with
532 assistance with RNA extractions. We are grateful to Dr Kevin Rozwadowski (Agriculture and
533 Agri-Food Canada) for the provision of pSKI106.

534 ## CONTRIBUTIONS

535 Y.K.S., S.M.S., G.R.F. and M.T.W. conceived and designed the research; Y.K.S., A.S., J.Y., K.M.
536 and M.T.W. performed the experiments; Y.K.S. and M.T.W. analysed the data; Y.K.S., S.M.S.
537 and M.T.W. wrote the manuscript.

538 ## SUPPLEMENTARY INFORMATION

539 **Supplementary Figure 1** Germination of *Brassica tournefortii* seed treated with karrikins

540 **Supplementary Figure 2** Extended phylogeny of eu-KAI2 and D14 proteins in angiosperms

541 **Supplementary Figure 3** Alignment of Brassica KAI2 sequences

542 **Supplementary Figure 4** BtD14a is functionally homologous to AtD14

543 **Supplementary Figure 5** Expression of BtKAI2 homologues in Arabidopsis and tobacco

544 **Supplementary Figure 6** Germination profiles of transgenic Arabidopsis seeds expressing
545 BtKAI2 homologues

546 **Supplementary Figure 7** BtKAI2a and BtKAI2b do not respond to karrikins in DSF assays

547 **Supplementary Table 1** List of sequences identified in this study

548 **Supplementary Table 2** List of oligonucleotides

549 ## FIGURE LEGENDS

550 **Figure 1. *Brassica tournefortii* is highly sensitive to KAR_1, the major karrikin analogue**
551 **isolated from smoke**

552 **a**, Germination responses of *B. tournefortii* seed to KAR_1 and KAR_2. Data are means ± SE; n = 3
553 biological replicates per treatment, ≥35 seeds per replicate. **b**, Levels of karrikin-responsive
554 transcripts *BtDLK2* and *BtSTH7* in *B. tournefortii* seed. Seed were imbibed for 24 hours in the
555 dark supplemented with KAR_1 or KAR_2. Transcripts were normalised to *BtCACS* reference
556 transcripts. Data are means ± SE, n = 3 biological replicates, ≥50 seeds per replicate. **c**,
557 Degradation of BtKAI2 protein levels in *B. tournefortii* seeds treated with KAR_1 or KAR_2 for 24,

558 48, and 72 hours. For each sample, 30 µg total protein isolated from imbibed seeds was
559 separated by SDS-PAGE, blotted, and challenged with anti-KAI2 antibody. The reference panel
560 shows the blot stained by amido black. Samples from *A. thaliana* ecotype L*er* and *kai2-2*
561 seedlings serve as controls for antibody specificity. **d**, Hypocotyl elongation responses of *B.*
562 *tournefortii* seedlings treated with KAR_1 or KAR_2. Data are means ± SE of n = 3 biological
563 replicates, ≥12 seedlings per replicate. Scale bar: 10 mm.

564 **Figure 2. Two differentially expressed *B. tournefortii KAI2* homologues are functional in**
565 ***Arabidopsis***

566 **a**, Maximum likelihood phylogeny of KAI2 homologues in the Brassicaceae, based on
567 nucleotide data. Node values represent bootstrap support from 100 replicates. A eu-KAI2
568 sequence from *Gossypium raimondii* (Malvaceae) serves as an outgroup. Tree shown is a
569 subset of a larger phylogeny in Supplementary Fig. 2. **b**, Transcript levels of the three *BtKAI2*
570 homologues in seed imbibed for 24 h (left) and four-day-old seedlings (right) treated with or
571 without 1 µM KAR_1 for 24 h. **c**, Seedling and rosette phenotypes of two independent
572 transgenic lines of Arabidopsis homozygous for *KAI2pro:GFP-BtKAI2x* transgenes. Scale bars:
573 5 mm (upper); 50 mm (lower). **d**, Immunoblots of soluble proteins challenged with antibodies
574 against KAI2 (upper panel), GFP (middle panel) or actin (lower panel). Non-specific bands are
575 marked with asterisks. Protein was isolated from pools of approximately fifty 7-day-old
576 seedlings.

577 **Figure 3. Functional divergence between BtKAI2 homologues**
578 **a**, Germination responses of primary dormant *Arabidopsis* seed homozygous for *KAI2pro:GFP-*
579 *BtKAI2x* transgenes in the *kai2-2* background. Germination values were determined 120 h
580 after sowing. Extended germination curves are shown in Supplementary Fig. 6. Data are
581 means ± SE, n = 3 independent seed batches, 75 seed per batch. **b**, Hypocotyl elongation
582 responses of *KAI2pro:GFP-BtKAI2x* seedlings treated with KAR_1 or KAR_2. Data are means ± SE
583 of n = 3 biological replicates, 12–18 seedlings per replicate. **c**, Levels of *DLK2* transcripts in 8-
584 day-old *KAI2pro:GFP-BtKAI2x* seedlings treated with KAR_1 or KAR_2 for eight hours. Expression
585 was normalised to *CACS* reference transcripts and scaled to the value for mock-treated
586 seedlings within each genotype. Data are means ± SE of n = 3 biological replicates. Pairwise
587 significant differences: * $P < 0.05$ ** $P < 0.01$ *** $P < 0.001$; ns, $P > 0.05$ (ANOVA).

588 **Figure 4. Two residues account for ligand specificity between BtKAI2a and BtKAI2b**

589 **a**, DSF curves of SUMO-BtKAI2a and SUMO-BtKAI2b fusion proteins treated with 0-50 μM
590 GR24$^{ent\text{-}5DS}$, a KAI2-bioactive ligand. Each curve is the average of three sets of reactions, each
591 comprising four technical replicates. Insets plot the minimum value of –(dF/dT) at the melting
592 point of the protein as determined in the absence of ligand (means ± SE, n = 3). Significant
593 differences from untreated control: * $P < 0.05$ ** $P < 0.01$ *** $P < 0.001$ (ANOVA). **b–d**, Solved
594 structure of AtKAI2 (PDB: 3w06 [36]) (**b**) and derived homology models (**c–d**) of BtKAI2a and
595 BtKAI2b. Coloured surfaces depict internal cavities; values indicate the volumes of the
596 primary ligand-binding cavities, adjacent to the catalytic Ser-His-Asp residues. Also shown is a
597 variable secondary pocket, to the left of the primary pocket in these images. **e**, DSF curves of
598 SUMO-BtKAI2a(b) and SUMO-BtKAI2b(a) fusion proteins treated with 0-50 μM GR24$^{ent\text{-}5DS}$. **f**,
599 Levels of *DLK2* transcripts (normalized to *CACS* reference transcripts) in two independent
600 lines of *KAI2pro:GFP-BtKAI2a* and *-BtKAI2b* seedlings treated for two hours with 0.1 μM
601 GR24$^{ent\text{-}5DS}$. Data are means ± SE; n = 3 biological replicates. Letters indicate significantly
602 different groupings (ANOVA; $P < 0.05$).

603 SUPPLEMENTARY FIGURE LEGENDS

604 **Supplementary Figure 1. Germination of *Brassica tournefortii* seed treated with**
605 **karrikins**
606 **a**, Structures of KAR_1, KAR_2 and two enantiomers of GR24. **b**, Germination response of the
607 "Merridin" batch of *B. tournefortii* seed treated with KAR_1 and KAR_2 after three days. **c-d**,
608 Germination response of the "Perth" batch to KAR_1 (**c**) and KAR_2 (**d**). Data in Figure 1a are
609 derived from the data shown in **c**. **e-f**, Rates of KAR_1 and KAR_2 uptake by imbibed seed, as
610 determined by GC-MS.

611 **Supplementary Figure 2. Extended phylogeny of eu-KAI2 and D14 proteins in**
612 **angiosperms**
613 Maximum likelihood phylogeny of KAI2 and D14 homologues in the Brassicaceae and
614 monocots, based on nucleotide data. Node values represent bootstrap support from 100
615 replicates. A KAI2 sequence from *Selaginella moellendorffii* (SmKAI2a; Waters et al. 2015)
616 serves as an outgroup for the eu-KAI2 clade.

617 **Supplementary Figure 3. Alignment of Brassica KAI2 sequences**
618 Full length protein coding regions of *KAI2* homologues from four *Brassica* species (*Brassica*
619 *tournefortii*, *B. rapa*, *B. nigra* and *B. oleracea*) were translated from database nucleic acid

620 sequences and aligned to Arabidopsis *KAI2* using MAFFT (Katoh et al, 2002) implemented in
621 Geneious R10 software (Biomatters Ltd). Residues that are unique to BtKAI2c but otherwise
622 invariant are highlighted with asterisks (*); residues 98 and 191 are highlighted with red
623 boxes.

624 **Supplementary Figure 4. BtD14a is functionally homologous to AtD14**
625 Three independent transgenic lines of Arabidopsis *Atd14-1* were analysed for functional
626 complementation of the mutant phenotype by an *AtD14pro:BtD14a* transgene. **a**, Rosette and
627 leaf morphology at 31 days post-germination. **b**, Plant height and number of primary rosette
628 branches at 45 days post-germination. **c**, Quantification of height and branching parameters, *n*
629 = 10 plants per genotype. Scale bars: 50 mm.

630 **Supplementary Figure 5. Expression of BtKAI2 homologues in Arabidopsis and tobacco**
631 **a**, Alignment of the protein regions corresponding to the peptide epitope TTNPDYFDFDRYSN
632 of AtKAI2, against which the anti-KAI2 peptide was raised. BtKAI2b, with a more divergent
633 epitope, is relatively poorly detected by the anti-KAI2 antibody (see Figure 2d). **b**, Transient
634 expression of BtKAI2a, BtKAI2b and BtKAI2c proteins in tobacco. Plasmids encoding N-
635 terminal, *c*-myc-tagged proteins were transferred to *Agrobacterium*, and the resulting strains
636 used to infiltrate tobacco leaves. After 96 h, samples were harvested in triplicate (two to three
637 leaves per sample). Mock-treated leaves were transformed with a plasmid encoding a non-
638 tagged protein. Sixty micrograms of total protein were separated by SDS-PAGE, blotted and
639 challenged with anti-*c*-myc antibody (Genscript A00704). Band intensity was measured using
640 ImageJ, and expression was normalised to intensity of the Rubisco large subunit (RbcL) band
641 on the "stain-free" gel imaged under UV light. Error bars indicate SE, *n* = 3 replicates. **c**,
642 Quantitative RT-PCR analysis of *GFP* and *DLK2* transcripts, normalised to *CACS* reference
643 transcripts. Data are derived from a single biological replicate with four technical PCR
644 replicates. RNA was isolated from approximately 50 seven-day-old seedlings per genotype,
645 and are the same samples as those shown in the immunoblots in Figure 2d.

646 **Supplementary Figure 6. Germination profiles of transgenic Arabidopsis seeds**
647 **expressing BtKAI2 homologues**
648 Freshly harvested seed (three batches per genotype, each batch harvested from four plants)
649 were removed from freezer storage, surface-sterilised and sown on 1% Phytagel
650 supplemented with 0.1% acetone (mock), 1 μM KAR_1 or 1 μM KAR_2. Seed were incubated
651 under constant light at 25 °C. Seed were examined for germination (radicle protrusion) 72 h

652 after sowing and every 24 h thereafter. Data are means ± SE of three independent seed
653 batches and 75 seed per batch. For each transgene, two independent, homozygous transgenic
654 lines were analysed. Data presented in Figure 3 of the main manuscript are derived from
655 these data.

656 **Supplementary Figure 7. BtKAI2a and BtKAI2b do not respond to karrikins in DSF**
657 **assays**
658 Differential scanning fluorimetry curves of BtKAI2a and BtKAI2b in presence of 0–200 μM
659 KAR_1 or KAR_2 (**a**) or the two enantiomers of GR24 (**b**). Data are means of eight technical
660 replicates at each concentration of ligand.

661

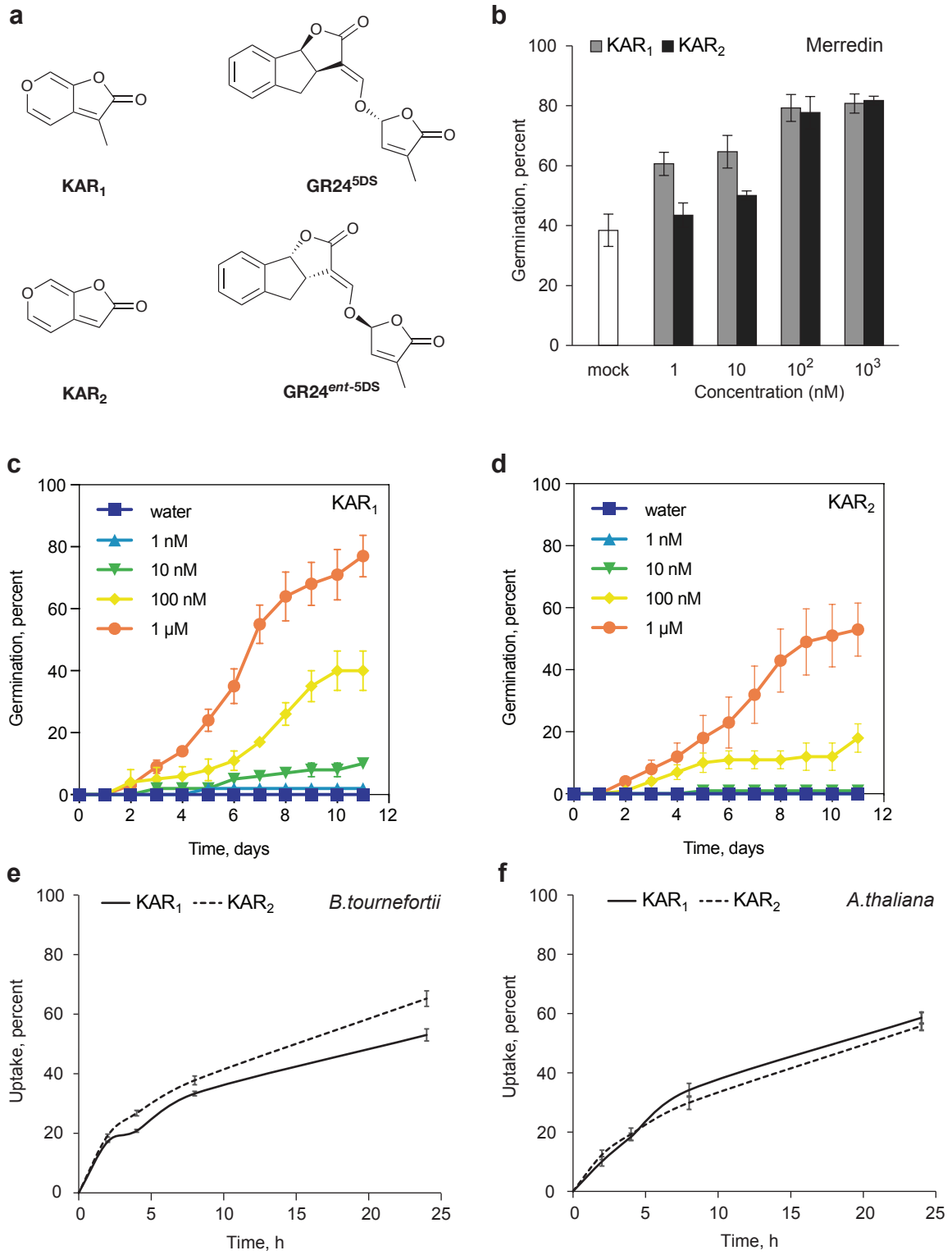

Supplementary Figure 1. Germination of *Brassica tournefortii* seed treated with karrikins
a, Structures of KAR_1, KAR_2 and two enantiomers of GR24. **b,** Germination response of the "Merridin" batch of *B. tournefortii* seed treated with KAR_1 and KAR_2 after three days. **c-d,** Germination response of the "Perth" batch to KAR_1 (**c**) and KAR_2 (**d**). Data in Figure 1a are derived from the data shown in **c.** **e-f**, Rates of KAR_1 and KAR_2 uptake by imbibed seed, as determined by GC-MS.

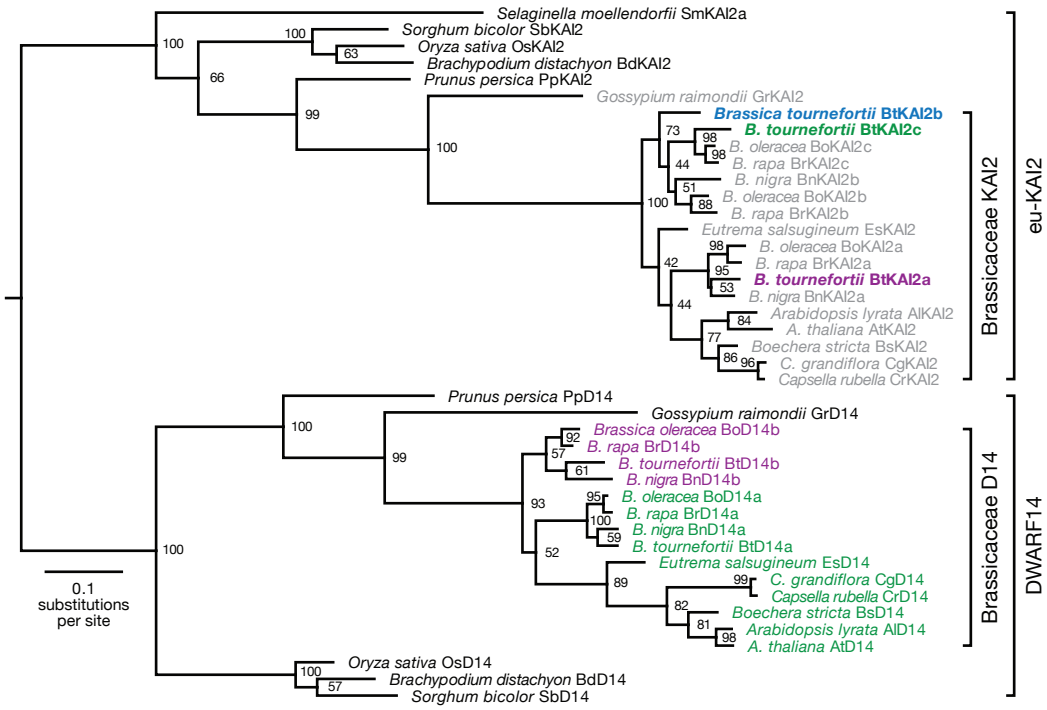

Supplementary Figure 2. Extended phylogeny of eu-KAI2 and D14 proteins in angiosperms
Maximum likelihood phylogeny of KAI2 and D14 homologues in the Brassicaceae and monocots, based on nucleotide data. Node values represent bootstrap support from 100 replicates. A KAI2 sequence from *Selaginella moellendorffii* (SmKAI2a; Waters et al. 2015) serves as an outgroup for the eu-KAI2 clade.

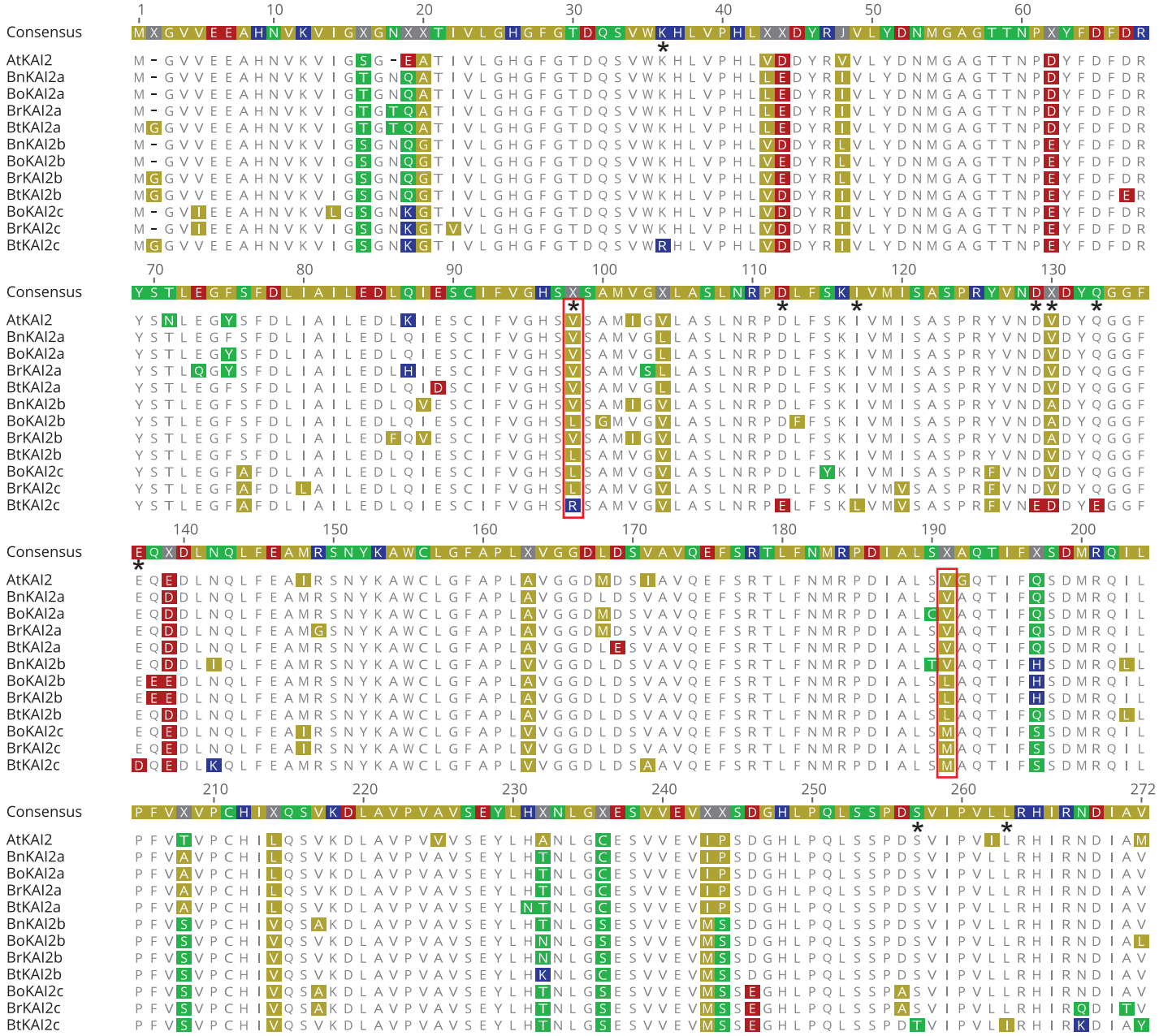

Supplementary Figure 3. Alignment of *Brassica* KAI2 sequences

Full length protein coding regions of KAI2 homologues from four *Brassica* species (*Brassica tournefortii*, *B. rapa*, *B. nigra* and *B. oleracea*) were translated from database nucleic acid sequences and aligned to Arabidopsis KAI2 using MAFFT (Katoh et al, 2002) implemented in Geneious R10 software (Biomatters Ltd). Residues that are unique to BtKAI2c but otherwise invariant are highlighted with asterisks (*); residues 98 and 191 are highlighted with red boxes.

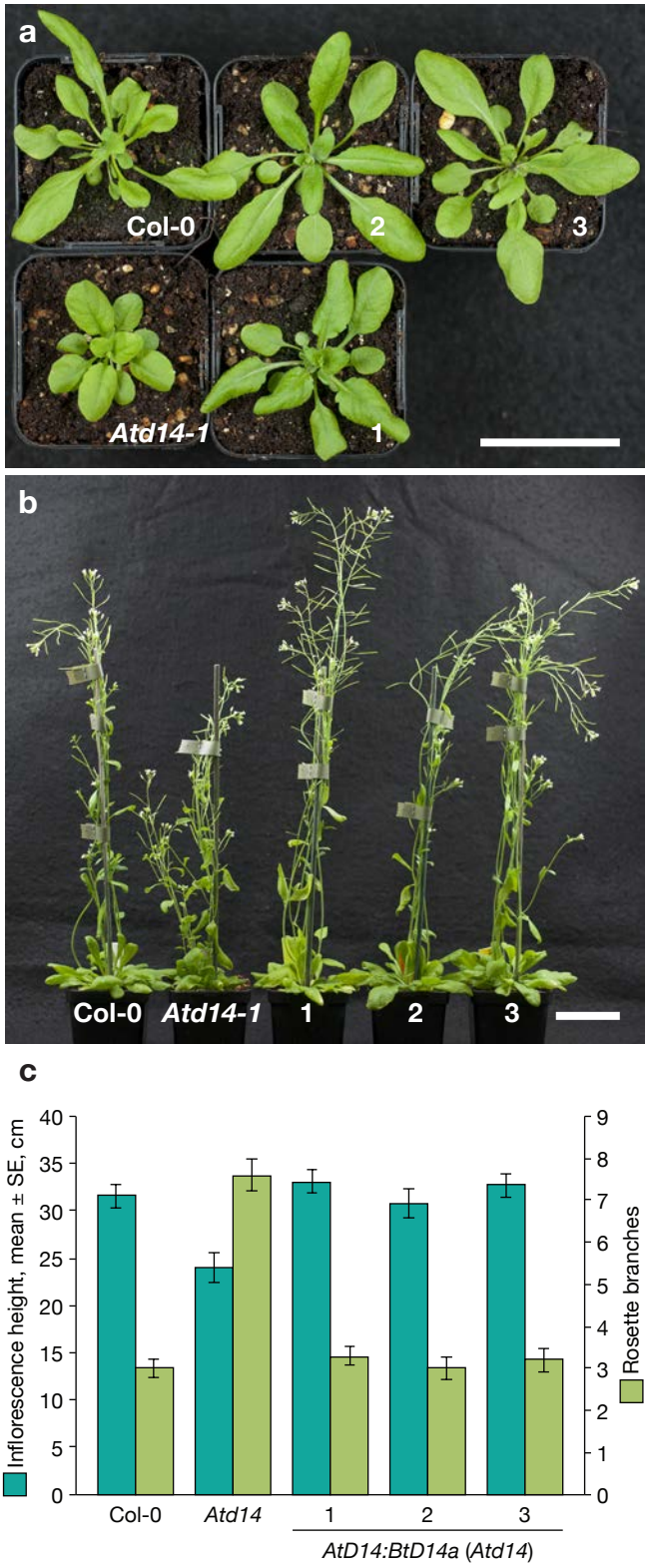

Supplementary Figure 4. BtD14a is functionally homologous to AtD14
Three independent transgenic lines of Arabidopsis *Atd14-1* were analysed for functional complementation of the mutant phenotype by an *AtD14pro:BtD14a* transgene. **a**, Rosette and leaf morphology at 31 days post-germination. **b**, Plant height and number of primary rosette branches at 45 days post-germination. **c**, Quantification of height and branching parameters, *n* = 10 plants per genotype. Scale bars: 50 mm.

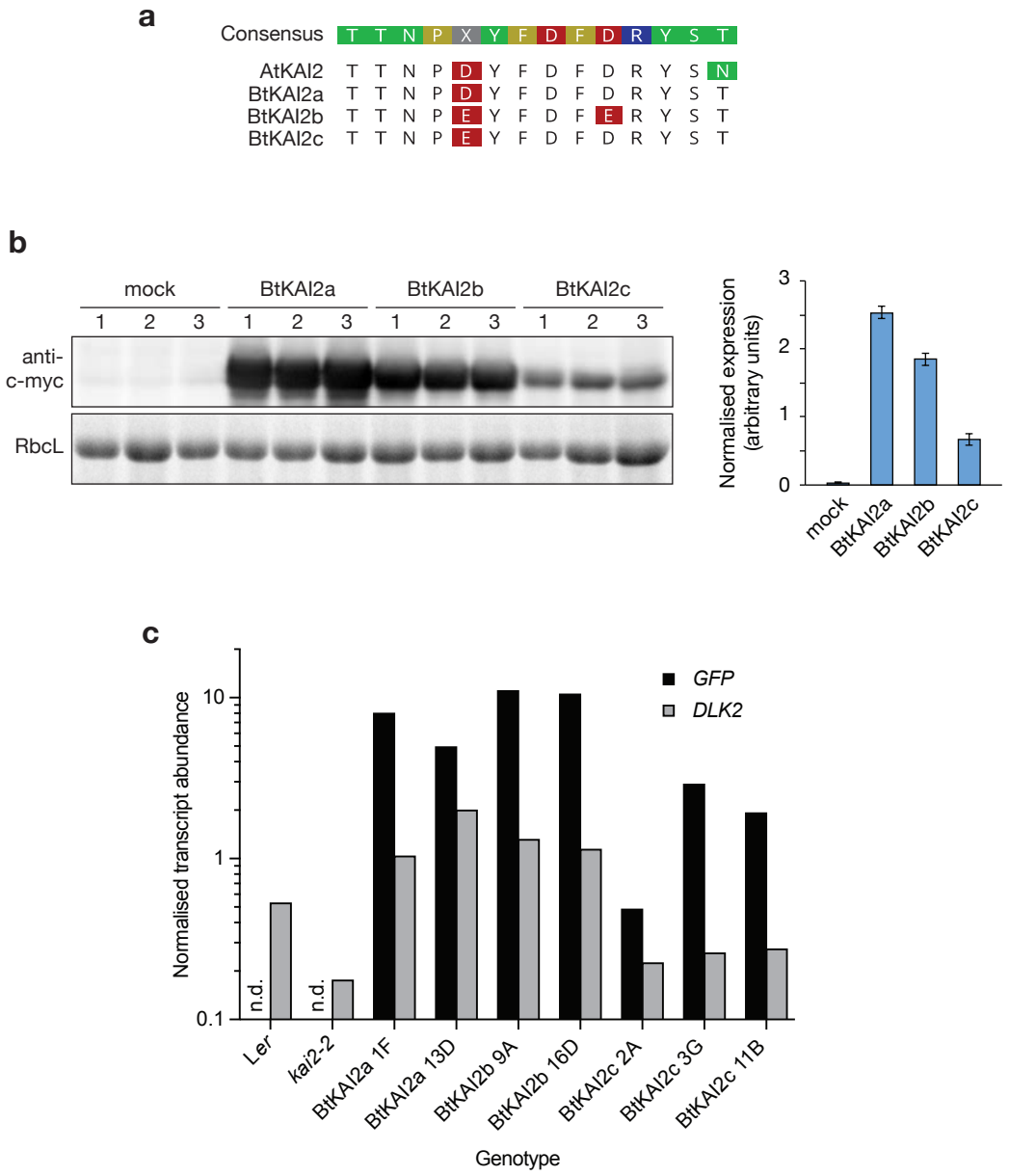

Supplementary Figure 5. Expression of BtKAI2 homologues in Arabidopsis and tobacco
a, Alignment of the protein regions corresponding to the peptide epitope TTNPDYFDFDRYSN of AtKAI2, against which the anti-KAI2 peptide was raised. BtKAI2b, with a more divergent epitope, is relatively poorly detected by the anti-KAI2 antibody (see Figure 2). **b**, Transient expression of BtKAI2a, BtKAI2b and BtKAI2c proteins in tobacco. Plasmids encoding N-terminal, c-myc-tagged proteins were transferred to Agrobacterium, and the resulting strains used to infiltrate tobacco leaves. After 96 h, samples were harvested in triplicate (two to three leaves per sample). Mock-treated leaves were transformed with a plasmid encoding a non-tagged protein. Sixty micrograms of total protein were separated by SDS-PAGE, blotted and challenged with anti-c-myc antibody (Genscript A00704). Band intensity was measured using ImageJ, and expression was normalised to intensity of the Rubisco large subunit (RbcL) band on the “stain-free” gel imaged under UV light. Error bars indicate SE, n = 3 replicates. **c**, Quantitative RT-PCR analysis of *GFP* and *DLK2* transcripts, normalised to *CACS* reference transcripts. Data are derived from a single biological replicate with four technical PCR replicates. RNA was isolated from approximately 50 seven-day-old seedlings per genotype, and are the same samples as those shown in the immunoblots in Figure 2.

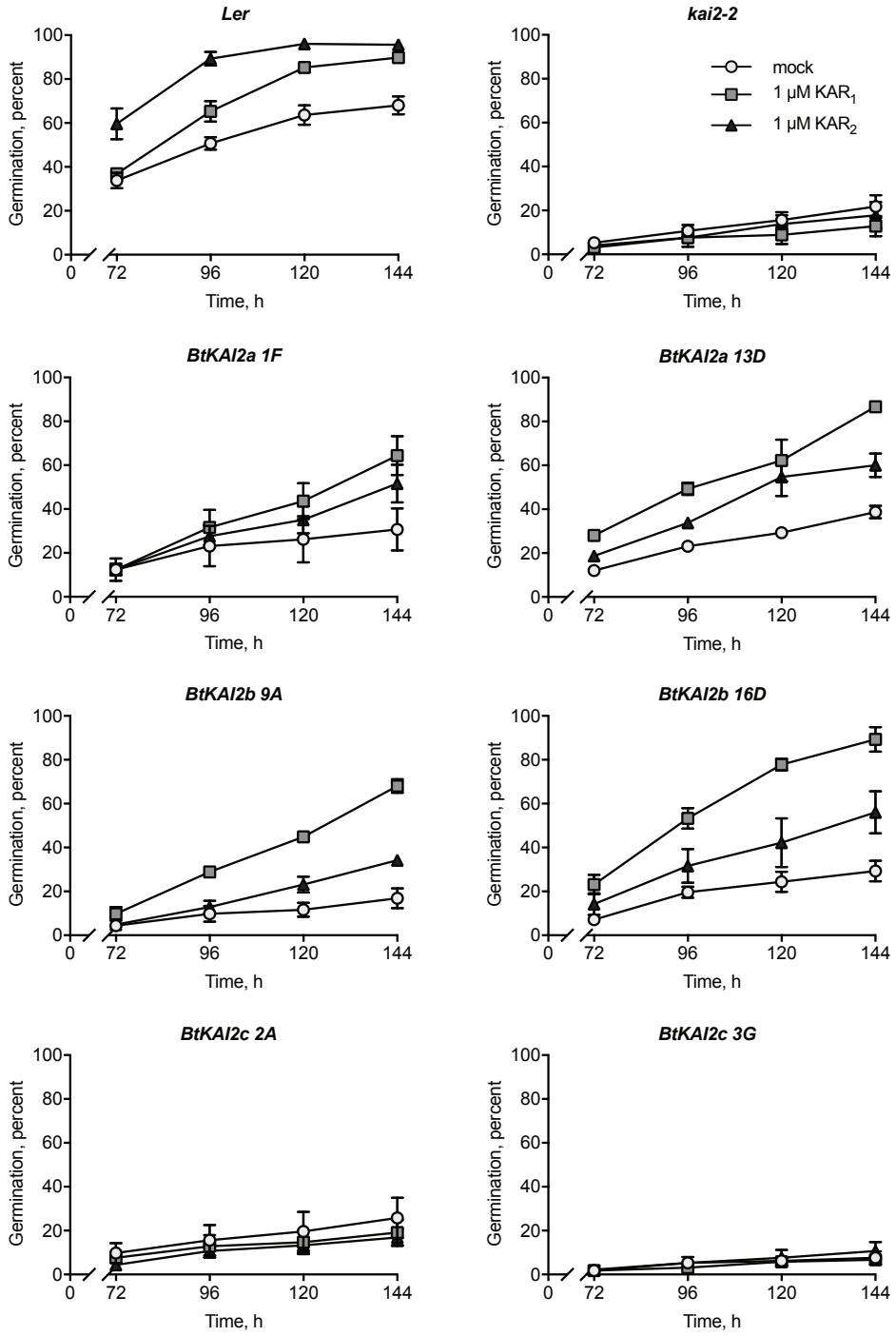

Supplementary Figure 6. Germination profiles of transgenic Arabidopsis seeds expressing BtKAI2 homologues Freshly harvested seed (three batches per genotype, each batch harvested from four plants) were removed from freezer storage, surface-sterilised and sown on 1% Phytagel supplemented with 0.1% acetone (mock), 1 μM KAR_1 or 1 μM KAR_2. Seed were incubated under constant light at 25 °C. Seed were examined for germination (radicle protrusion) 72 h after sowing and every 24 h thereafter. Data are means ± SE of three independent seed batches and 75 seed per batch. For each transgene, two independent, homozygous transgenic lines were analysed. Data presented in Figure 3 of the main manuscript are derived from these data.

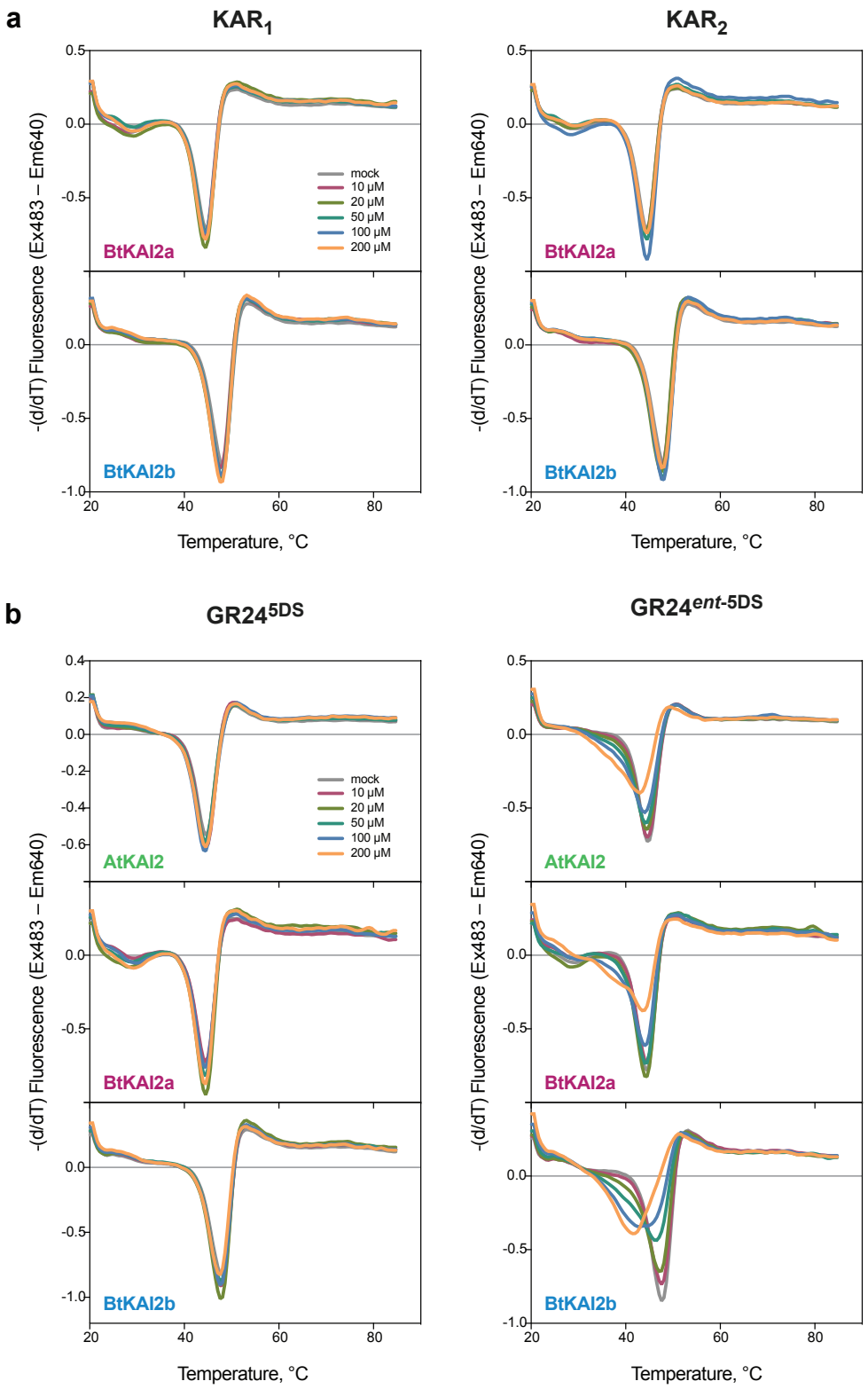

Supplementary Figure 7. BtKAI2a and BtKAI2b do not respond to karrikins in DSF assays
Differential scanning fluorimetry curves of BtKAI2a and BtKAI2b in presence of 0–200 µM KAR_1 or KAR_2 (**a**) or the two enantiomers of GR24 (**b**). Data are means of eight technical replicates at each concentration of ligand.

Supplementary Table 1. List of sequences identified in this study

KAI2

Species	Gene name	Sequence ID	Source	Reference
Arabidopsis lyrata	*AlKAI2*	AL7G13320.t1	Phytozome	This work
Arabidopsis thaliana	*AtKAI2*	At3g37470	TAIR	Waters et al (2012)
Brassica tournefortii (saharan mustard)	*BtKAI2a*	MG783328	GenBank/NCBI	This work
Brassica tournefortii (saharan mustard)	*BtKAI2b*	MG783329	GenBank/NCBI	This work
Brassica tournefortii (saharan mustard)	*BtKAI2c*	MG783330	GenBank/NCBI	This work
Brassica rapa (field mustard, AA genome)	*BrKAI2a*	XM_009111126.2	GenBank/NCBI	This work
Brassica rapa (field mustard, AA genome)	*BrKAI2b*	XM_009140247	GenBank/NCBI	This work
Brassica rapa (field mustard, AA genome)	*BrKAI2c*	XM_009144693	GenBank/NCBI	This work
Brassica nigra (black mustard, BB genome)	*BnKAI2a*	LFLV01000699.1	GenBank/NCBI	This work
Brassica nigra (black mustard, BB genome)	*BnKAI2b*	LFLV01001772.1	GenBank/NCBI	This work
Brassica oleracea (cabbage, CC genome)	*BoKAI2a*	XM_013766720.1	Phytozome	This work
Brassica oleracea (cabbage, CC genome)	*BoKAI2b*	XM_013738288.1	Phytozome	This work
Brassica oleracea (cabbage, CC genome)	*BoKAI2c*	XM_013778816.1	Phytozome	This work
Boechera stricta	*BsKAI2*	Bostr.30440s0001.1	Phytozome	This work
Capsella rubella	*CrKAI2*	Carubv10005485m	Phytozome	This work
Capsella grandiflora	*CgKAI2*	Cagra.1232s0005.1	Phytozome	This work
Eutrema salsugineum	*EsKAI2*	Thalv10025969m	Phytozome	Bythell-Douglas et al (2017)
Gossypium raymondii	*GrKAI2*	Gorai.003G028500.1	Phytozome	Bythell-Douglas et al (2017)
Prunus persica	*PpKAI2*	Ppa009957m	Phytozome	Bythell-Douglas et al (2017)
Brachypodium distachyon	*BdKAI2*	Bradi1g15880.1	Phytozome	Bythell-Douglas et al (2017)
Oryza sativa	*OsKAI2*	Os03g32270.1	Phytozome	Bythell-Douglas et al (2017)
Sorghum bicolor	*SbKAI2*	Sorbic.001G330000.1	Phytozome	Bythell-Douglas et al (2017)
Selaginella moellendorffii	*SmKAI2a*	Selmo_441991	Phytozome	Waters et al (2015)

D14

Species	Gene name	Sequence ID	Source	Reference
Arabidopsis lyrata	*AlD14*	AL3G13900.t1	Phytozome	This work
Arabidopsis thaliana	*AtD14*	AT3G03990.1	TAIR	Waters et al (2012)
Brassica oleracea (cabbage, CC genome)	*BoD14a*	LOC106343216	Phytozome	This work
Brassica oleracea (cabbage, CC genome)	*BoD14b*	LOC106343689	Phytozome	This work
Brassica nigra (black mustard, BB genome)	*BnD14a*	LFLV01002090	GenBank/NCBI	This work
Brassica nigra (black mustard, BB genome)	*BnD14b*	LFLV01000699	GenBank/NCBI	This work
Brassica rapa (field mustard, AA genome)	*BrD14a*	Brara.A03790	Phytozome	This work
Brassica rapa (field mustard, AA genome)	*BrD14b*	Brara.E03476	Phytozome	This work
B. tournefortii (saharan mustard)	*BtD14a*	MG783331	Phytozome	This work
B. tournefortii (saharan mustard)	*BtD14b*	MG783332	Phytozome	This work
Boechera stricta	*BsD14*	Bostr.2570s0310	Phytozome	This work
Capsella grandiflora	*CgD14*	Cagra.15970s0001	Phytozome	This work
Capsella rubella	*CrD14*	Carubv10014401m	Phytozome	This work
Eutrema salsugineum	*EsD14*	Thhalv10021292m	Phytozome	Bythell-Douglas et al (2017)
Gossypium raymondii	*GrD14*	Gorai.010G025600.1	Phytozome	Bythell-Douglas et al (2017)
Prunus persica	*PpD14*	ppa010005m	Phytozome	Bythell-Douglas et al (2017)
Brachypodium distachyon	*BdD14*	Bradi1g70930.3	Phytozome	Bythell-Douglas et al (2017)
Oryza sativa	*OsD14*	Os03g10620.1	Phytozome	Bythell-Douglas et al (2017)
Sorghum bicolor	*SbD14*	Sobic.001G465100.1	Phytozome	Bythell-Douglas et al (2017)

DLK2

Species	Gene name	Sequence ID	Source	Reference
B. tournefortii (saharan mustard)	*BtDLK2*	MG783333	GenBank/NCBI	This work

Supplementary Table 2. Oligonucleotides used in this study

Oligonucleotide	Sequence	Notes
Cloning		
BtD14a_F	AAAAAAGCAGGCTTCCATTATGAGTCAACACAACAT	BtD14a
BtD14a_R	CAAGAAAGCTGGGTTTTAAAGTCACCGAGGAAG	BtD14a
BtKAI2_universal_F	GGGGACAAGTTTGTACAAAAAAGCAGGCTTCATGGGAGGTGTGGTAGAGGA	All BtKAI2
RACE_R	GGGGACCACTTTGTACAAGAAAGCTGGGTCATTCTCAATAGACAATAGAC	BtKAI2a
Contig1_R	GGGGACCACTTTGTACAAGAAAGCTGGGTCCGAAACGACCCACTCACTTACC	BtKAI2b
Contig5_R	GGGGACCACTTTGTACAAGAAAGCTGGGTCCGAAGCAGAACCAAGCTAA	BtKAI2c
BtKAI2-SUMO-Gib_F	TGAGGCTCACCGCGAACAGATTGGAGGTATGGGAGGTGTGGTAGAGGAAG	pSUMO-BtKAI2a / BtKAI2b
BtKAI2a-SUMO-Gib_R	CGGATCTCAGTGGTGGTGGTGGTGGTGCTCAGACAGCGATGTCATTACGA	pSUMO-BtKAI2a
BtKAI2b-SUMO-Gib_R	CGGATCTCAGTGGTGGTGGTGGTGGTGCTCATACAGCAATGTCGTTGCGG	pSUMO-BtKAI2b
BtKAI2b_L98V_F1	ATCTTTGTTGGTCACTCTGTCTCCGCCATG	For BtKAI2b(a) mutagenesis
BtKAI2b_L191V_R1	TTTGGAAAATGGTCTGAGCCACGGAGAGTG	For BtKAI2b(a) mutagenesis
BtKAI2b_L191V_F2	TCTCCGTGGCTCAGACCATTTTCCAAAGC	For BtKAI2b(a) mutagenesis
BtKAI2b_L98V_R2	CATGGCGGAGACAGAGTGACCAACAAAG	For BtKAI2b(a) mutagenesis
BtKAI2a_V98L_F1	ATCTTTGTTGGTCACTCTCTCTCCGCCATG	For BtKAI2a(b) mutagenesis
BtKAI2a_V191L_R1	TTTGGAAAATGGTCTGAGCCAGGGAGAGAG	For BtKAI2a(b) mutagenesis
BtKAI2a_V191L_F2	TCTCCCTGGCTCAGACCATTTTCCAAAG	For BtKAI2a(b) mutagenesis
BtKAI2a_V98L_R2	CATGGCGGAGAGAGAGTGACCAACAAAG	For BtKAI2a(b) mutagenesis
Quantitative PCR		
STH7_qF	CATCTCCGGTTCTCTCTCACTTCT	Designed against At4g39070
STH7_qR	CATTCTCTGCATAGTATTGCTCTGTC	Designed against At4g39070
BtDLK2_qF	GCTGCTTCTCCCAGGTATATAA	BtDLK2
BtDLK2_qR	GAAAGCAACCGCCCAAGCC	BtDLK2
AtDLK2_qF	GCTGCTTCTCCAAGGTATATAA	Designed against At3g24420
AtDLK2_qR	GAAATCAACCGCCCAAGCT	Designed against At3g24420
KUF1_qF	AACCCGTCAGTCCGGTTTATGTG	Designed against At1g31350
KUF1_qR	AACGACGGATGACGGTAAAGAATCC	Designed against At1g31350
IAA6_qF	TTCGGCTGTCTTGGCATAGGAG	Designed against At1g52830
IAA6_qR	TTCACGATCCTCAGCCTCTTGC	Designed against At1g52830
BtKAI2_universal_qF	GGTCATCTTCCTCAGCTTAG	All BtKAI2
BtKAI2_a_qR1	CCATTAATTTAATTTAAAATCACTTCCC	BtKAI2a
BtKAI2_b_qR1	GCATTTAATTTCGCTAAAACTCTTG	BtKAI2b
BtKAI2_c_qR1	GAAACGATATACTCAGTACTTACCAC	BtKAI2c
CACS_qF	ACTCAGGAAGGTGTACGGTCA	Designed against At5g46630
CACS_qR	TGCATTTGGAACAGGTTTGT	Designed against At5g46630